

Alpha cluster structures in light hypernuclei

Yasuro Funaki (RIKEN)

The 3rd Korea–Japan Workshop on Nuclear and Hadron Physics at J-PARC, @ Inha University, Korea, March 20–21, 2014.

Nuclear clustering

**Alpha particle condensation
typical example of nuclear clustering**

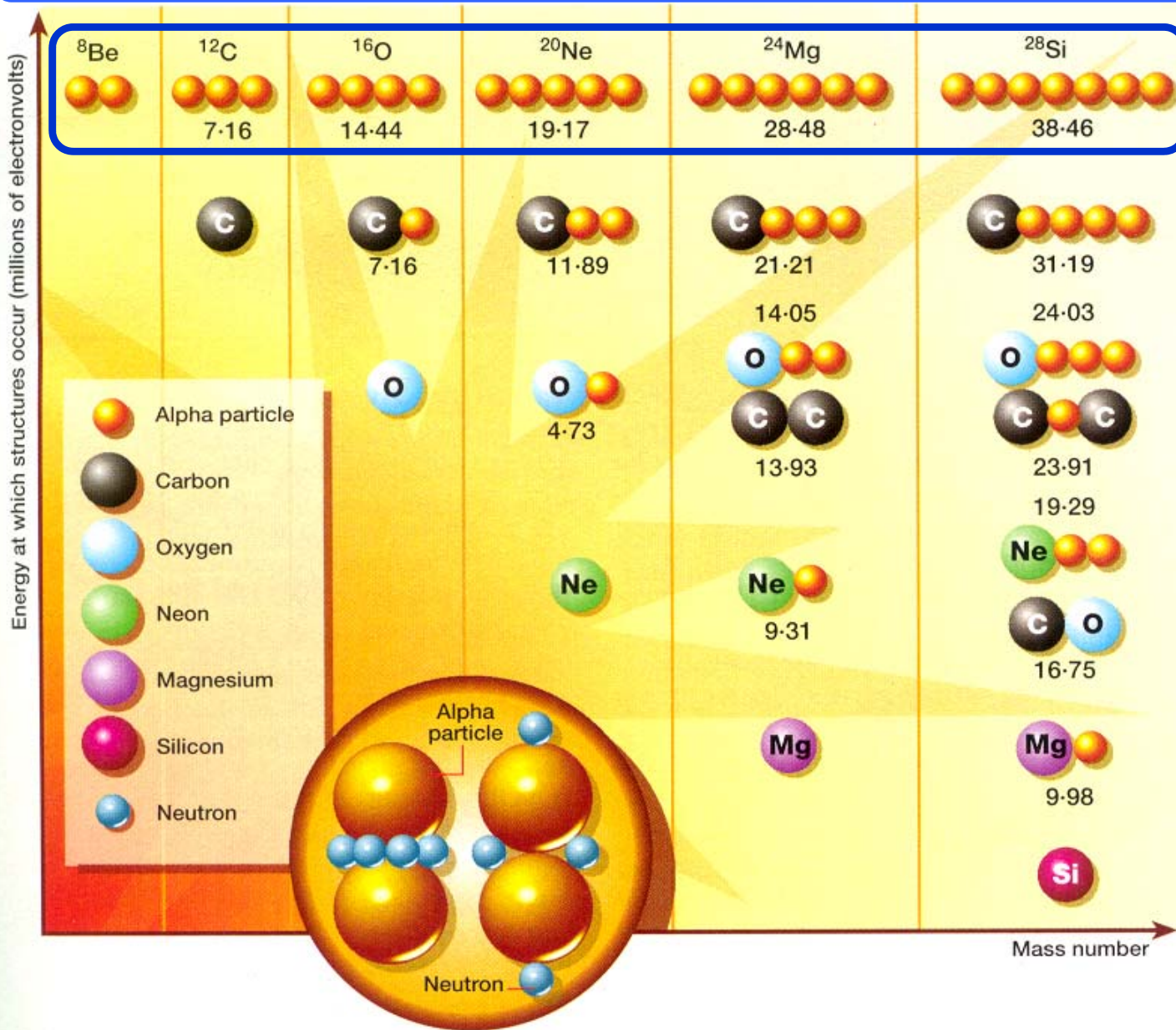
One of the most important recent progresses in nuclear cluster physics

“Container” picture of nuclear clustering

“Gaslike” cluster states to non-gaslike cluster states

- **Inversion doublet band states in ^{20}Ne**
- **3α and 4α linear-chain states**
- **$^9_{\Lambda}\text{Be}$ and $^{13}_{\Lambda}\text{C}$**

Prediction of cluster states in light nuclei (Ikeda Diagram)



← Limit of structural change from shell to clusters

The most tightly bound light cluster

α particle (quartet)

$E/A \sim 7 \text{ MeV}$ $E^* \sim 20 \text{ MeV}$
stiff

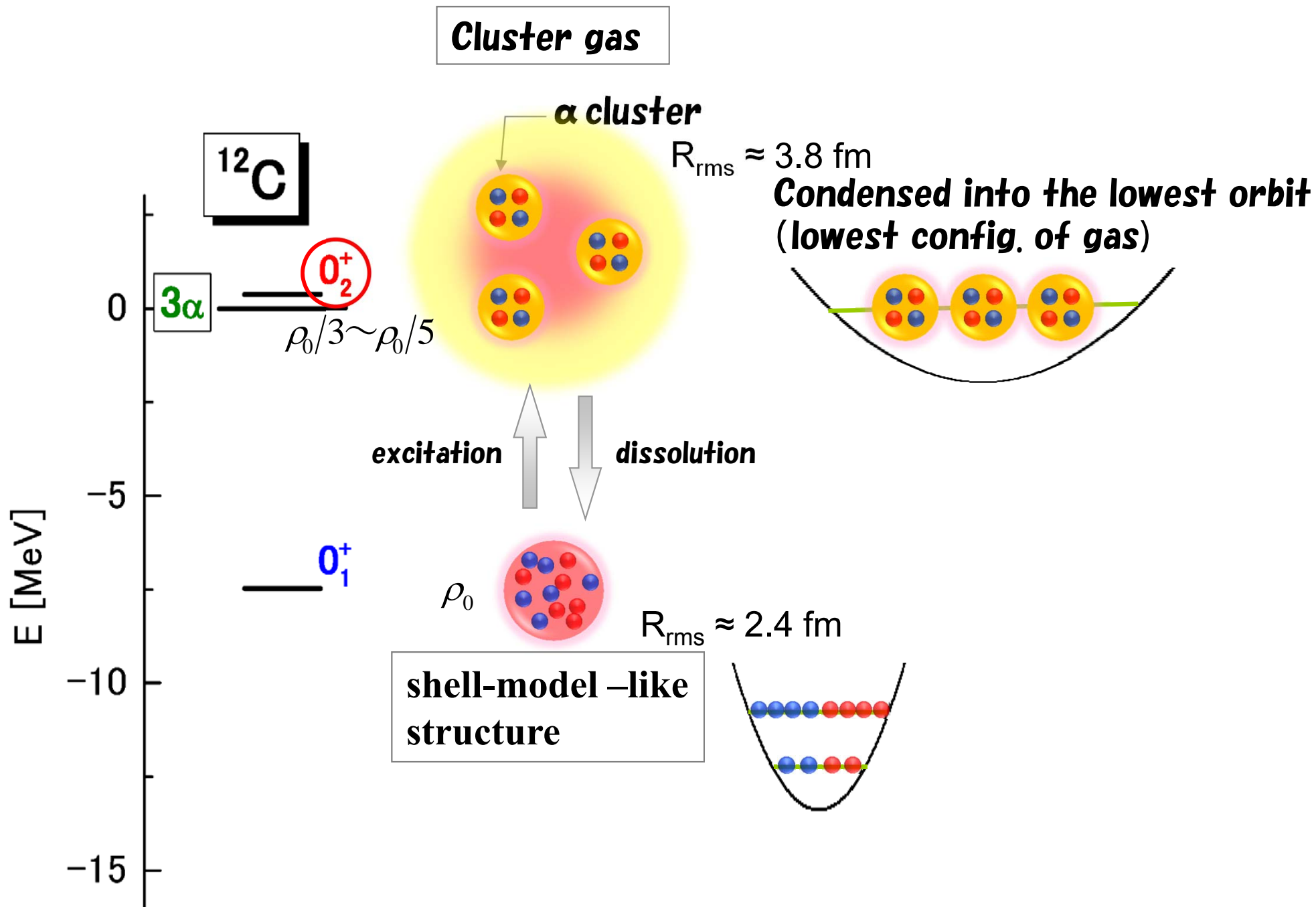
The most elemental subunit in nuclear cluster structures.

$E/A \sim 1 \text{ MeV}$

Classified according to the Threshold Rule.

K. Ikeda et al, PTP suppl. Extra num., 464 (1968).

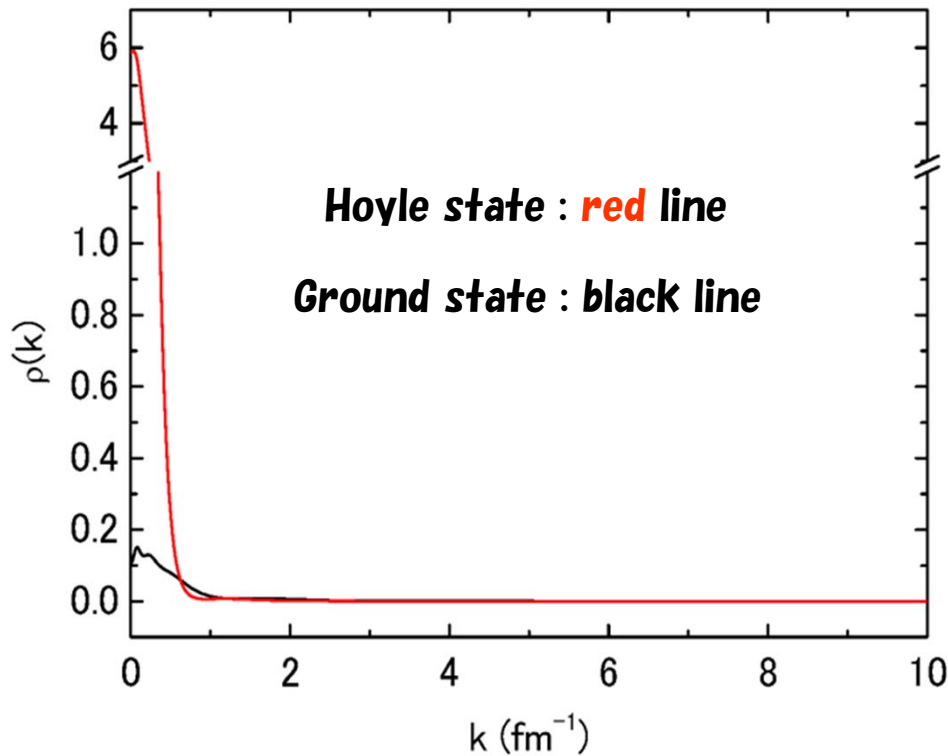
Alpha condensate state



3 α OCM (Orthogonality Condition Model)

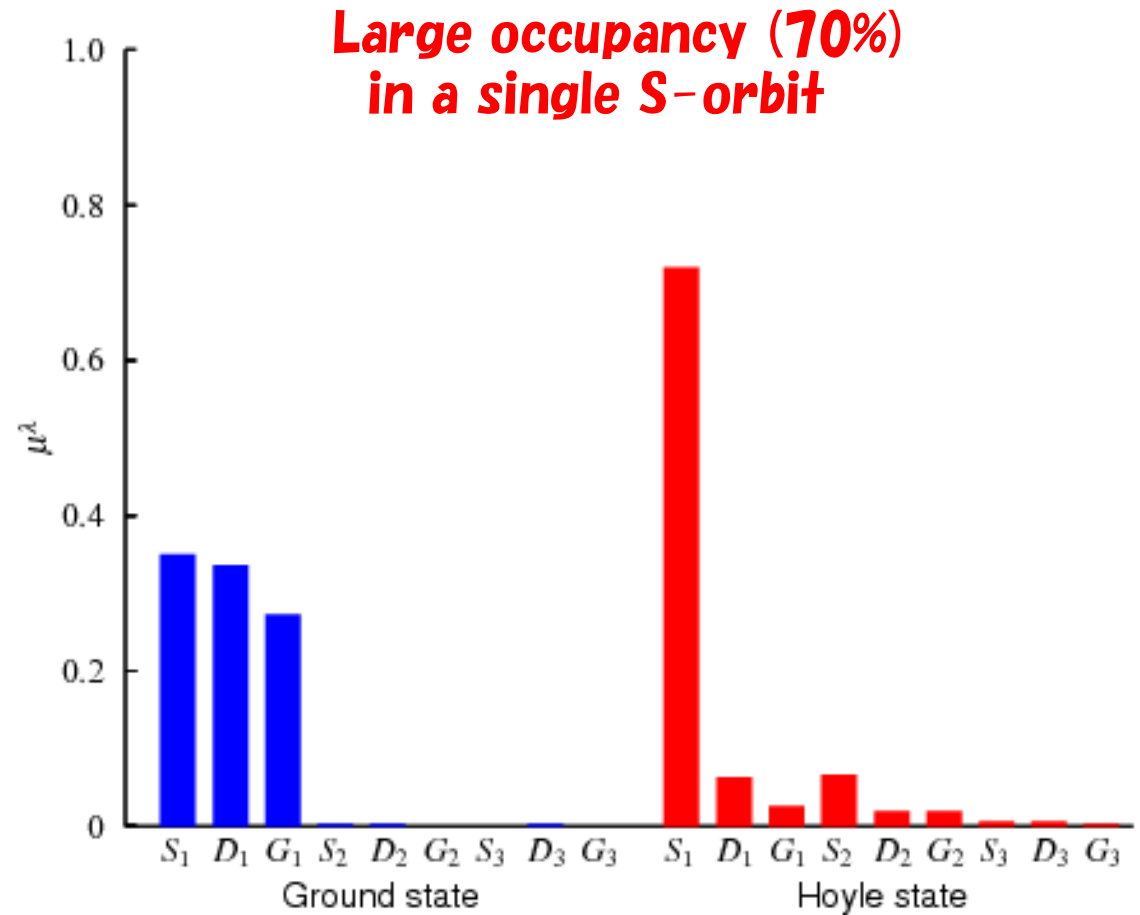
Direct information of alpha condensation

Momentum distribution of α - particle



**δ function -like peak
around zero momentum**

Occupation probability of single α - orbit

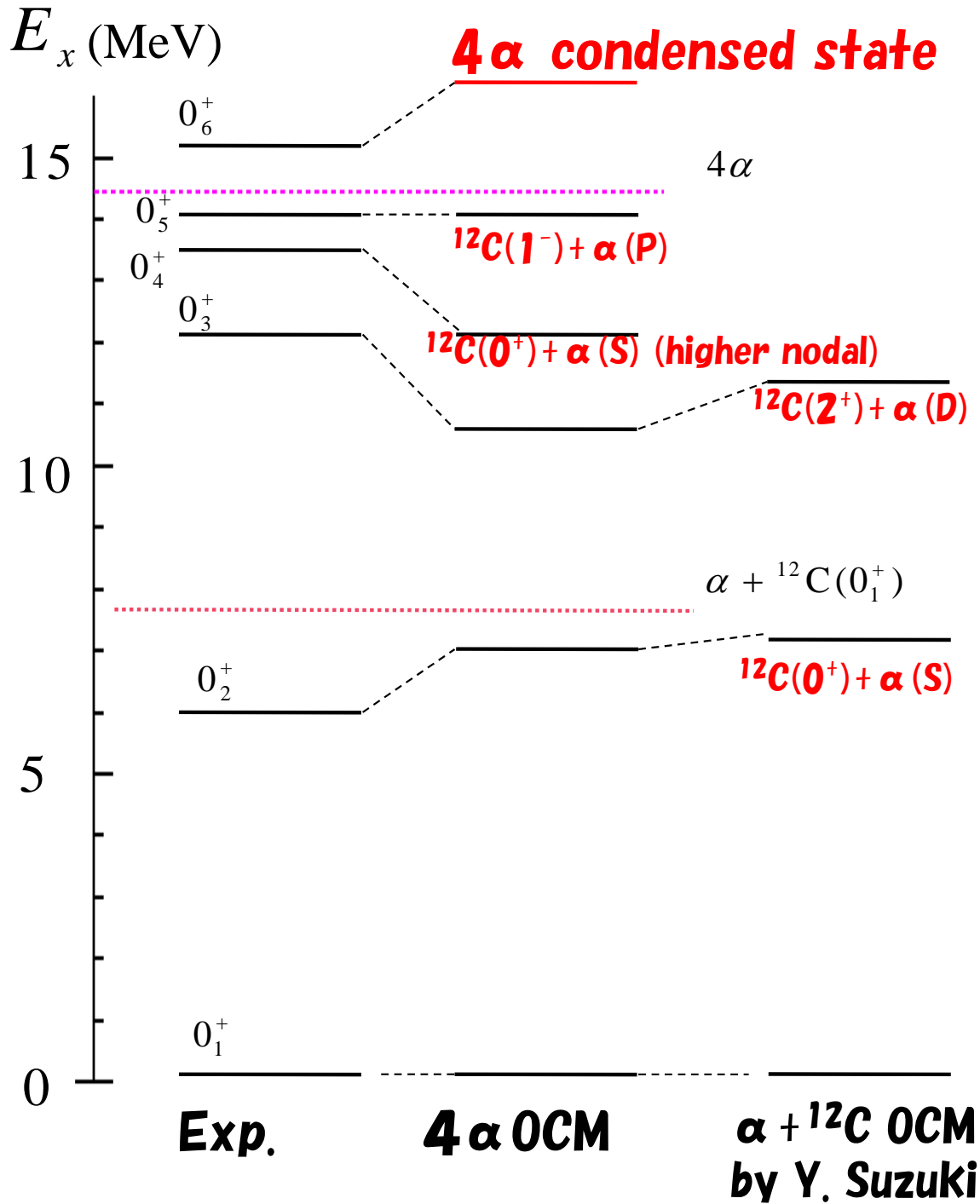


**Large occupancy (70%)
in a single S-orbit**

T. Yamada and P. Schuck, EPJA 26, 185 (2005).

See also H. Matsumura and Y. Suzuki, NPA 739, 238 (2004).

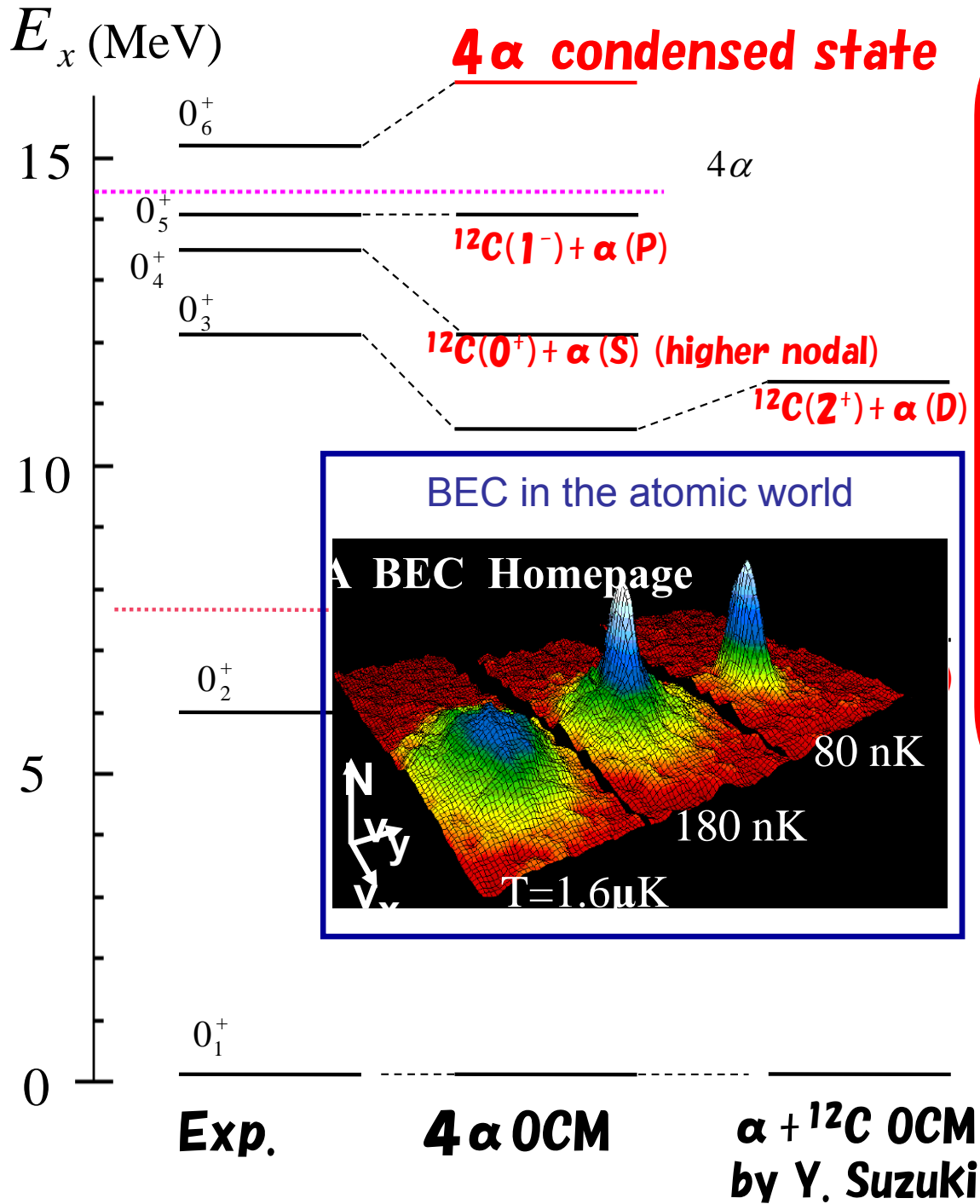
4-alpha condensate state in ^{16}O



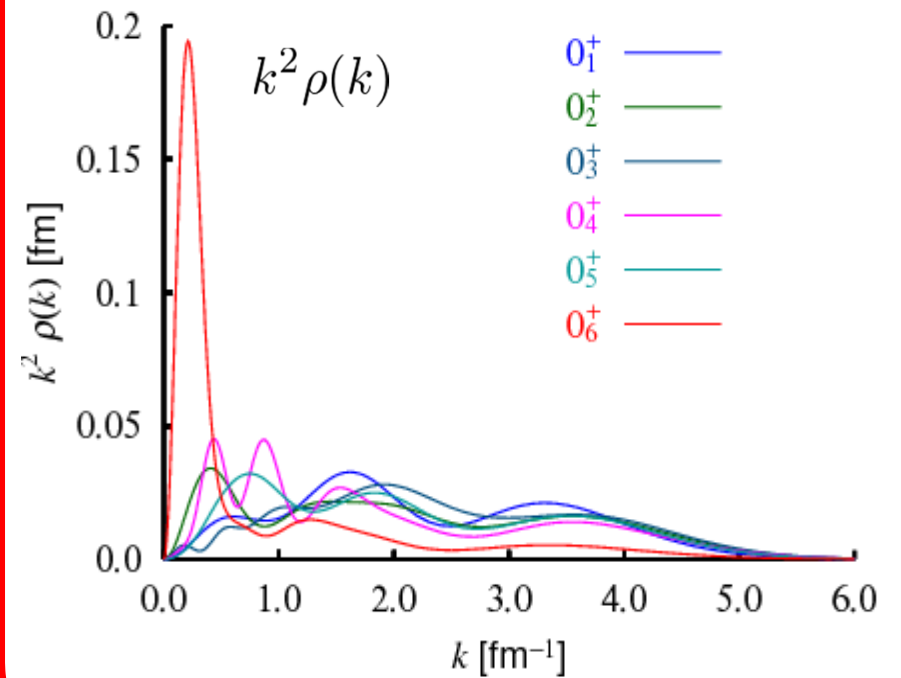
0_4^+ state: T. Wakasa, Y. F. et al.,
PLB 653, 173 (2007).

Y. F. et al., PRL 101, 081502 (2008).

4-alpha condensate state in ^{16}O



Momentum distributions of α particle



0_6^+ : 4α condensate

0_4^+ state: T. Wakasa, Y. F. et al., PLB 653, 173 (2007).

Y. F. et al., PRL 101, 081502 (2008).

THSR wave function : Alpha condensate-type wave function

Particle number projected BCS w.f.

$$\langle \mathbf{r}_1, \dots, \mathbf{r}_{2n} | \text{BCS} \rangle = \mathcal{A} \left\{ \Phi(\mathbf{r}_1, \mathbf{r}_2) \Phi(\mathbf{r}_3, \mathbf{r}_4) \cdots \Phi(\mathbf{r}_{2n-1}, \mathbf{r}_{2n}) \right\}$$

n α condensate w.f.

$$\langle \mathbf{r}_1, \dots, \mathbf{r}_{4n} | \Phi_{n\alpha} \rangle = \mathcal{A} \left\{ \Phi(\mathbf{r}_1, \mathbf{r}_2, \mathbf{r}_3, \mathbf{r}_4) \Phi(\mathbf{r}_5, \mathbf{r}_6, \mathbf{r}_7, \mathbf{r}_8) \cdots \Phi(\mathbf{r}_{4n-3}, \mathbf{r}_{4n-2}, \mathbf{r}_{4n-1}, \mathbf{r}_{4n}) \right\}$$

Variational ansatz (only one parameters B , or with deformation, $B_x = B_y, B_z$)

(THSR ansatz) A. Tohsaki, H. Horiuchi, P. Schuck and G. Röpke et al., PRL 87, 192501 (2001).

$$\Phi(\mathbf{r}_{4i-3}, \dots, \mathbf{r}_{4i}) = e^{-\frac{2}{B^2} (\mathbf{X}_i - \mathbf{X}_G)^2} \phi_\alpha(\mathbf{r}_{4i-3}, \dots, \mathbf{r}_{4i})$$

$$\phi_\alpha \propto e^{-\frac{1}{8b^2} \sum_{k < l} (\mathbf{r}_k - \mathbf{r}_l)^2}$$

c.o.m. of i -th α particle

$$\mathbf{X}_i = \frac{\mathbf{r}_{4i-3} + \dots + \mathbf{r}_{4i}}{4}$$

Total c.o.m.

$$\mathbf{X}_G = \frac{\mathbf{r}_1 + \dots + \mathbf{r}_{4n}}{4n}$$

THSR wave function : Alpha condensate-type wave function

Variational ansatz (only one parameters B , or with deformation, $B_x=B_y, B_z$)

(THSR ansatz) A. Tohsaki, H. Horiuchi, P. Schuck and G. Röpke et al., PRL **87**, 192501 (2001).

$$\Phi(\mathbf{r}_{4i-3}, \dots, \mathbf{r}_{4i}) = e^{-\frac{2}{B^2}(\mathbf{X}_i - \mathbf{X}_G)^2} \phi_\alpha(\mathbf{r}_{4i-3}, \dots, \mathbf{r}_{4i})$$

$$\phi_\alpha \propto e^{-\frac{1}{8b^2} \sum_{k < l} (\mathbf{r}_k - \mathbf{r}_l)^2}$$

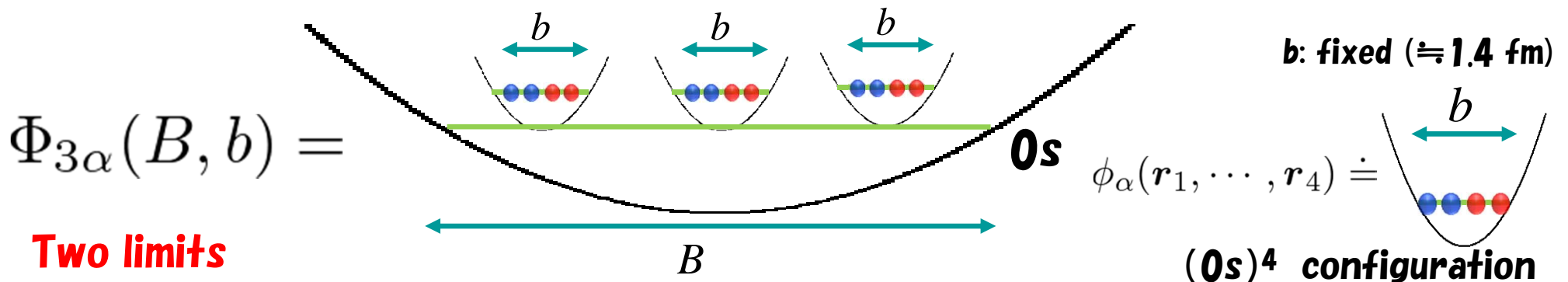
c.o.m. of i -th α particle

$$\mathbf{X}_i = \frac{\mathbf{r}_{4i-3} + \dots + \mathbf{r}_{4i}}{4}$$

Total c.o.m.

$$\mathbf{X}_G = \frac{\mathbf{r}_1 + \dots + \mathbf{r}_{4n}}{4n}$$

Pictorial image of the THSR wave function for $n=3$ (^{12}C)



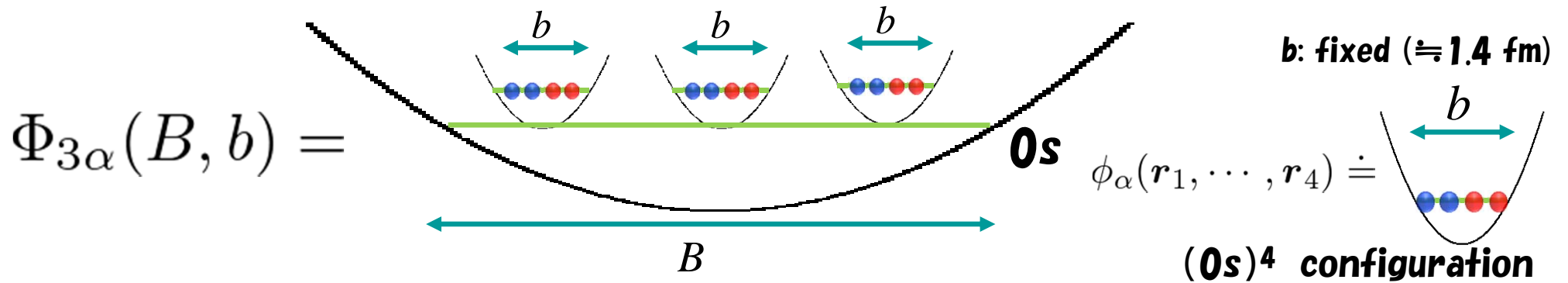
Two limits

$B = b$: Shell model w.f.

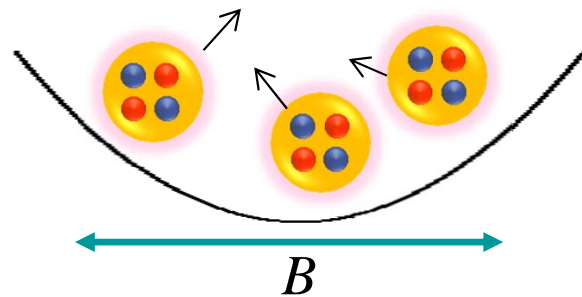
$B \gg b$: Gas of independent α -particles

THSR wave function : Alpha condensate-type wave function

Pictorial image of the THSR wave function for $n=3$ (^{12}C)



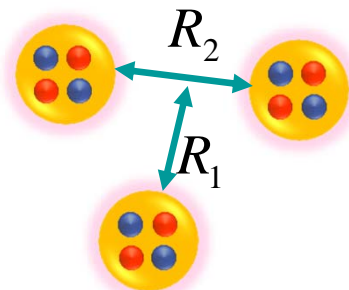
This, in general, gives ‘‘container’’ picture of nuclear clustering



Nonlocalized clustering

Characterized by a size parameter B of the container, corresponding to nuclear size.

Quite different from conventional picture of clustering



Localized clustering

Characterized by relative-distance parameters R 's between clusters.

For ${}^8\text{Be}$

Full 2α RGM solution, which is given by superposing many Brink w.fs, is completely equivalent to a single THSR w.f. (99.99%)

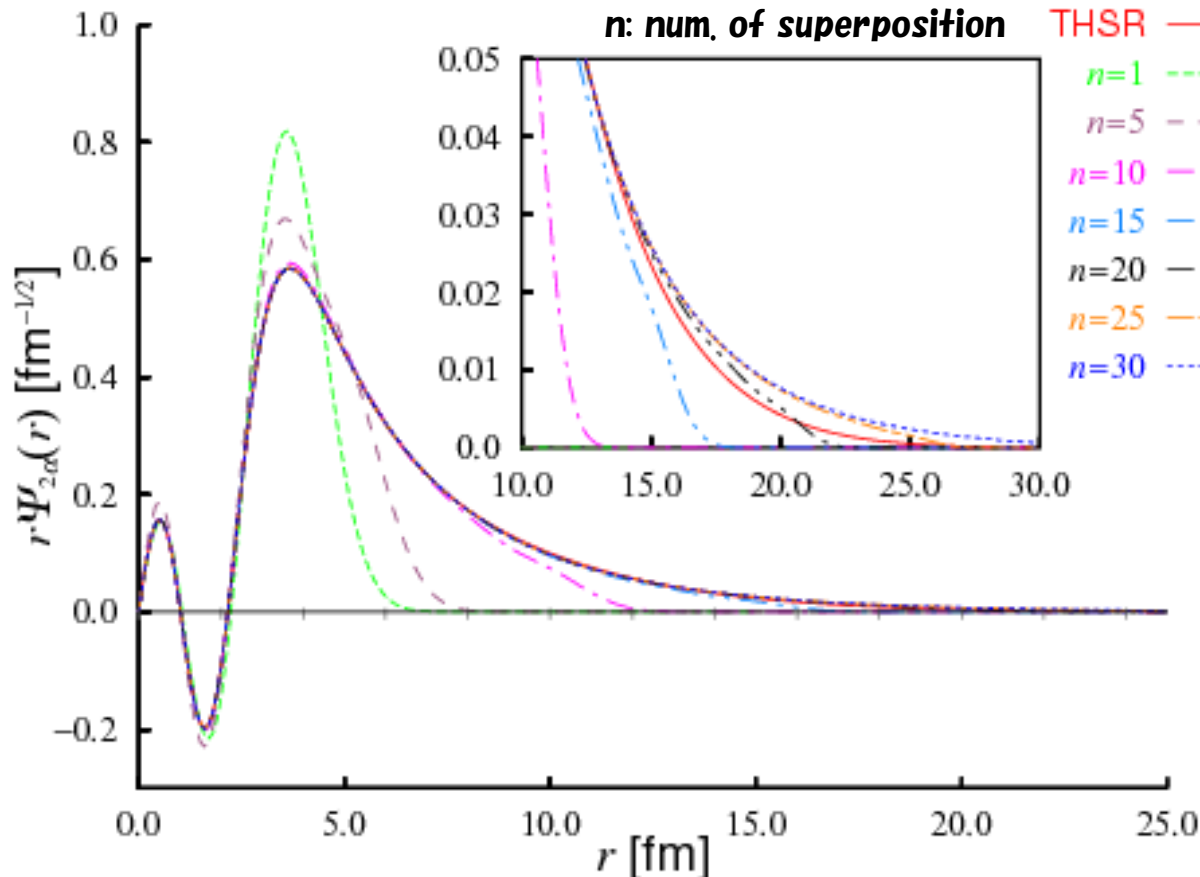
Y. F. et al., PTP 108, 297 (2002); PRC 80, 064326 (2009).

2α RGM eq.

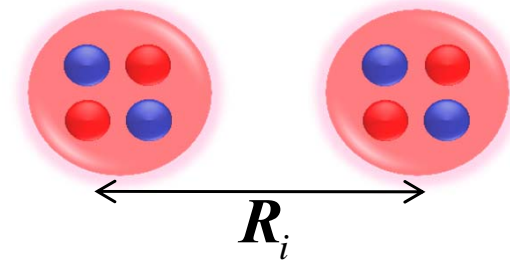
$$(H - EN)\chi = 0 \iff \left(\frac{1}{\sqrt{N}} H \frac{1}{\sqrt{N}} - E \right) \Psi_{2\alpha} = 0$$

$$\Psi_{2\alpha} = \sqrt{N}\chi = \int d^3b \sqrt{N(a,b)} \chi(b)$$

Relative w.f. between 2α particles



Superposition of dumbbells



$$\chi^{\text{Brink}}(\mathbf{r}) = \sum_{i=1}^n f(\mathbf{R}_i) \hat{P}_{J=0} \exp\left[-\frac{(\mathbf{r} - \mathbf{R}_i)^2}{b^2}\right]$$

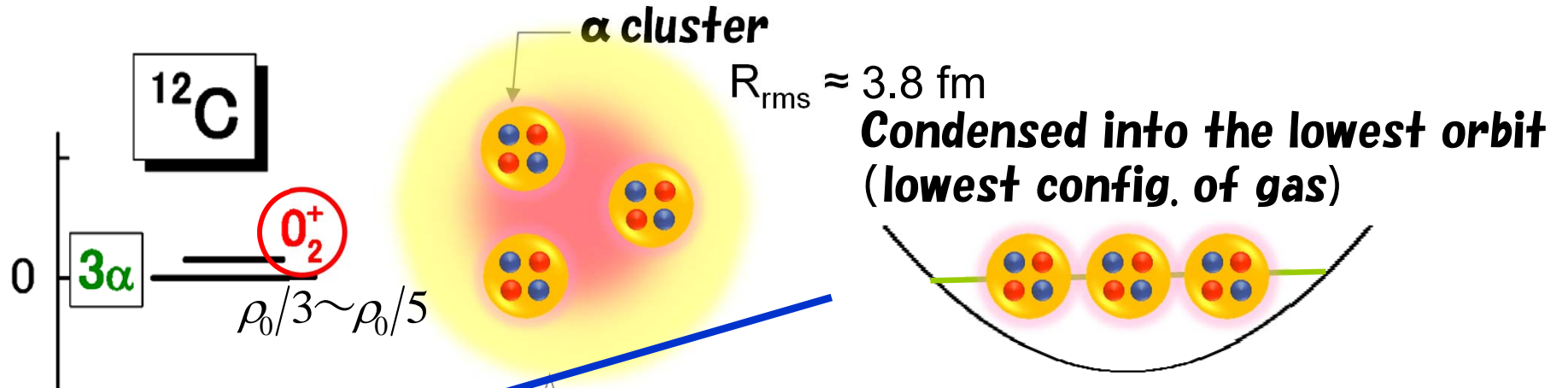
$$\Psi_{2\alpha}^{\text{Brink}} = \sqrt{N} \chi^{\text{Brink}}$$

The superposition of 30 Brink w.fs. coincides with one THSR ! $\left| \left\langle \Psi_{2\alpha}^{\text{Brink}} \mid \Psi_{2\alpha}^{\text{THSR}} \right\rangle \right|^2 = 0.9999$

First example of alpha cond. state

Y. F. et al, PRC 67, 051306(2003)

Cluster gas



3 α THSR w.f.

$$\hat{P}_{g.s.} \hat{P}_{J=0} \mathcal{A} \left\{ \prod_{i=1}^3 \chi_{3\alpha}^{THSR} (X_i - X_G : B_{\perp}, B_z) \phi_{\alpha_i} \right\} = \mathcal{A} \left\{ \chi_{3\alpha}^{RGM} (\xi_1, \xi_2) \phi_{\alpha_1} \phi_{\alpha_2} \phi_{\alpha_3} \right\}$$

$$\chi_{3\alpha}^{THSR} (X : B_{\perp}, B_z) = e^{-\frac{2}{B_{\perp}^2} (X_x^2 + X_y^2) - \frac{2}{B_z^2} X_z^2}$$

$${}^{RGM} \langle \phi_{\alpha_1} \phi_{\alpha_2} \phi_{\alpha_3} | H - E | \mathcal{A} \{ \chi_{3\alpha}^{RGM} (\xi_1, \xi_2) \phi_{\alpha_1} \phi_{\alpha_2} \phi_{\alpha_3} \} \rangle = 0$$

$(B_{\perp}, B_z) = (7.6 \text{ fm}, 2.5 \text{ fm})$ gives the very Hoyle state w.f.

This gives 99.3 % squared overlap with RGM w.f. (For ${}^8\text{Be}$, 99.99 % with 2 α RGM w.f.)

c.o.m. of i -th α particle

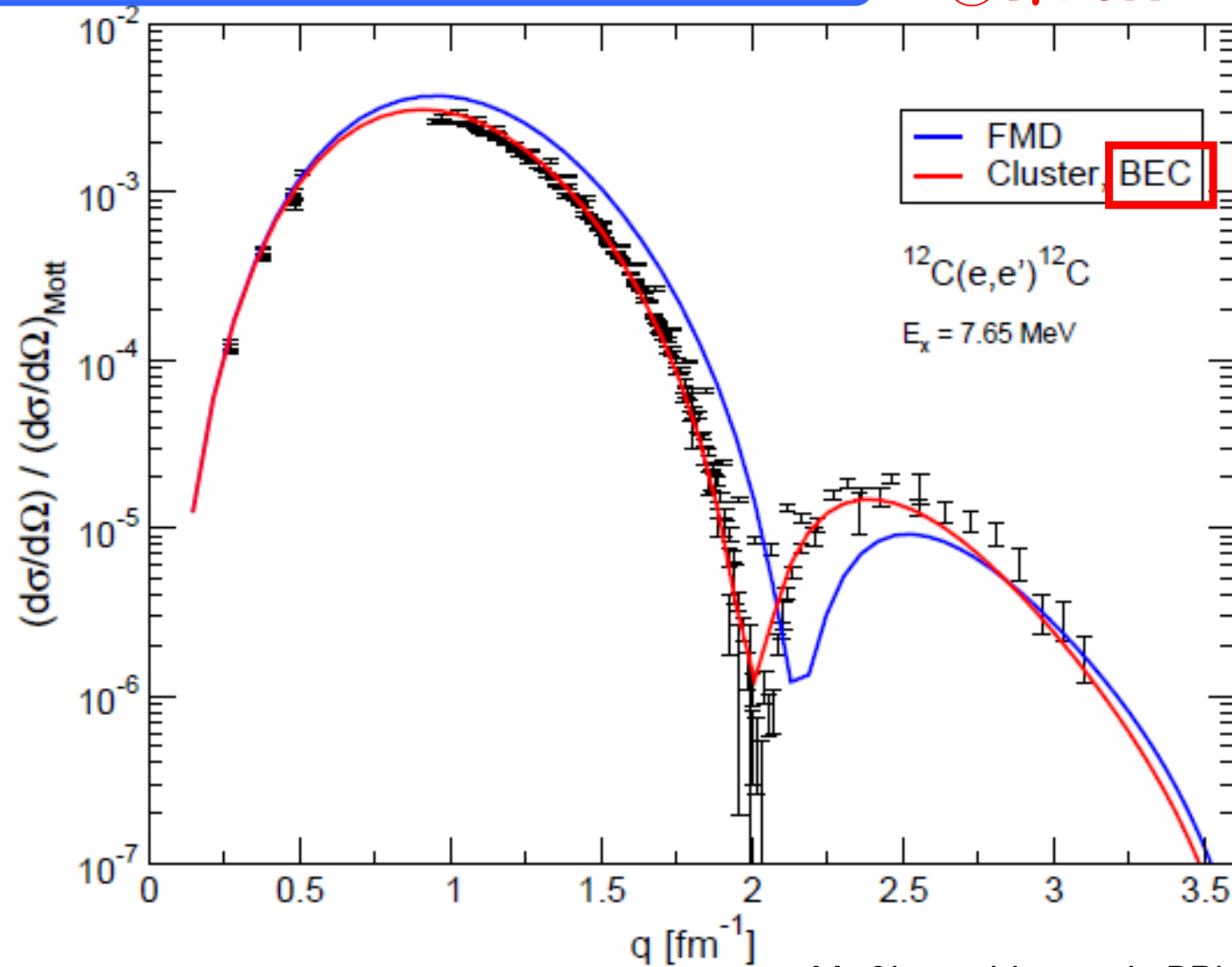
$$X_i = \frac{r_{4i-3} + \dots + r_{4i}}{4}$$

Total c.o.m.

$$X_G = \frac{r_1 + \dots + r_{4n}}{4n}$$

Electron Scattering Data ($0_1^+ \rightarrow 0_2^+$)

©T. Neff



M. Chernykh. et al., PRL 98, 032501 (2007)

Very nice reproduction by THSR w.f. (BEC)

Until now, we have thought that the single THSR w.f. is suitable for describing only gas-like cluster states such as represented by the alpha-condensate states.

For large (B_{\perp} , B_z)

However, this idea is completely misleading.

We pointed it out in new collaboration with Nanjing group.

Non-localized clustering: A new concept in nuclear clustering

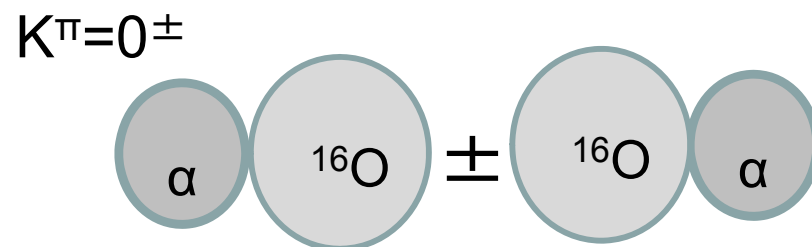
Bo Zhou (Nanjing), Zhongzhou Ren (Nanjing), Chang Xu (Nanjing)
Y. Funaki, T. Yamada, A. Tohsaki, H. Horiuchi, P. Schuck, G. Röpke

This opened a new horizon for nuclear cluster physics.

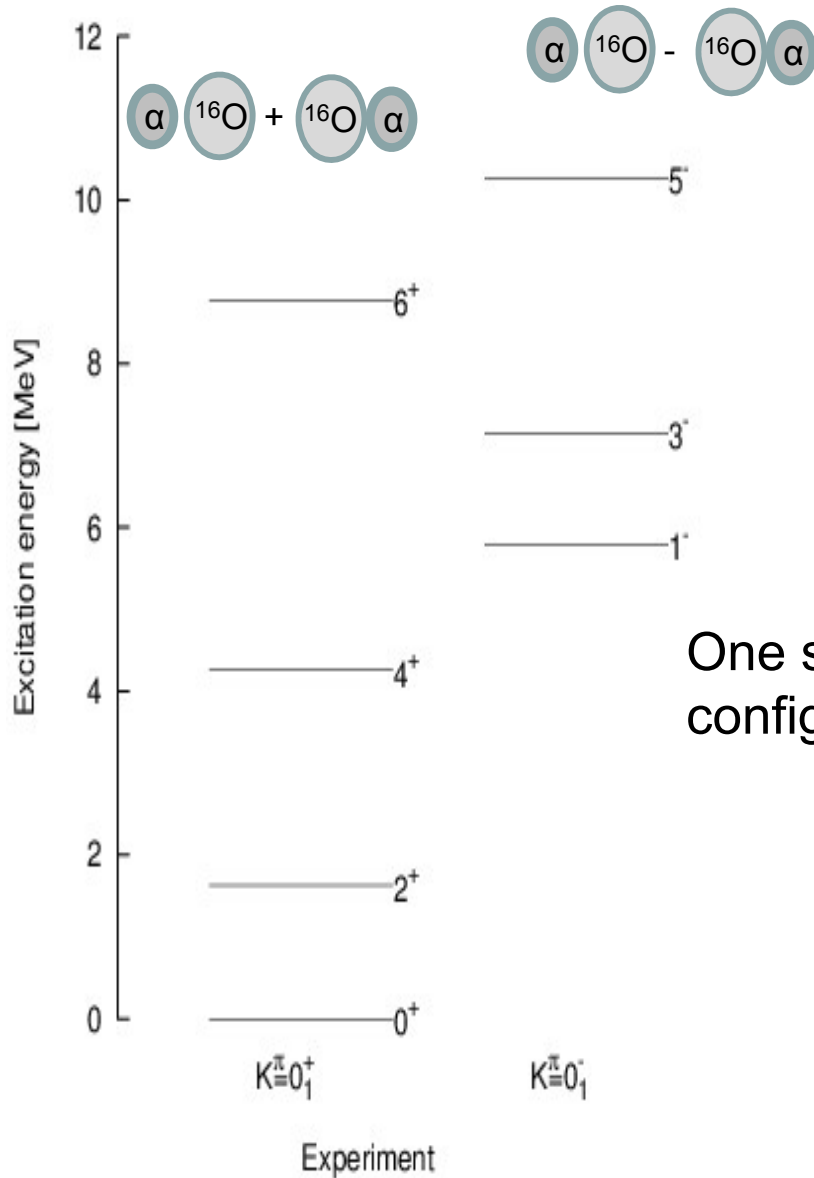
*B. Zhou, Y. F. et al., PRC86, 014301 (2012); PRL 110, 262501(2013);
arXiv:1310.7684(accepted from PRC)*

First example is the inversion doublet bands in ^{20}Ne .

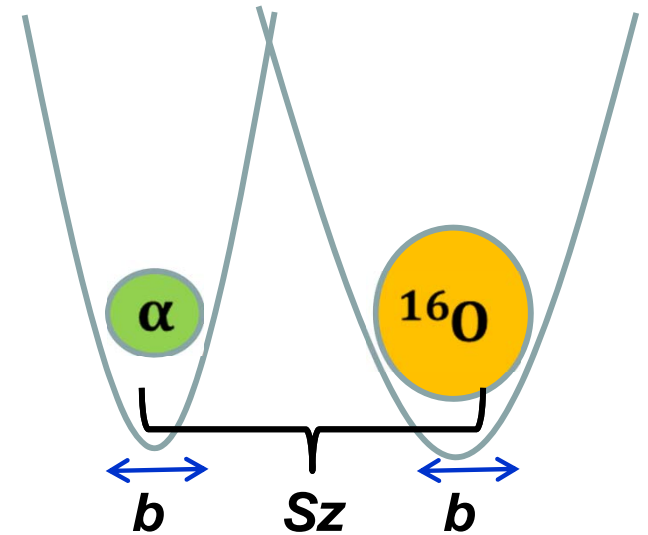
Localized clustering picture has been (had been) an important basis to understand them.



The energy levels of $\alpha+^{16}\text{O}$ inversion doublet bands in ^{20}Ne

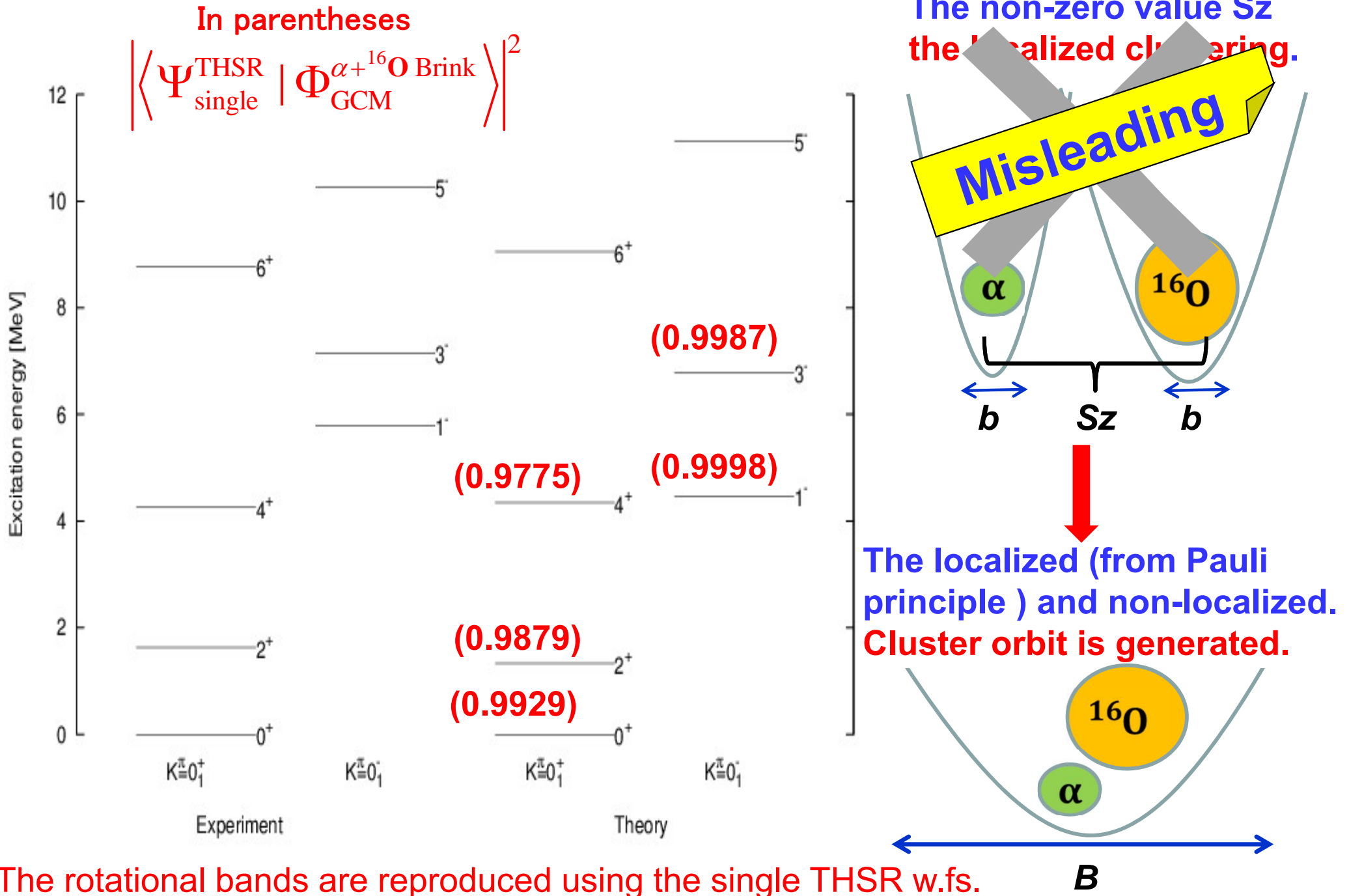


The non-zero value S_z
the localized clustering.



One should superpose many localized cluster configurations to reproduce the experimental spectrum

The energy levels of $\alpha+^{16}\text{O}$ inversion doublet bands in ^{20}Ne by THSR w.f.



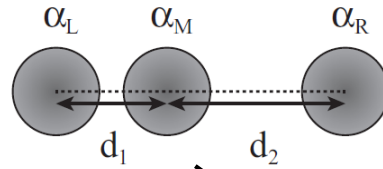
The rotational bands are reproduced using the single THSR w.fs.

The squared overlap with one-dim. THSR with single parameter

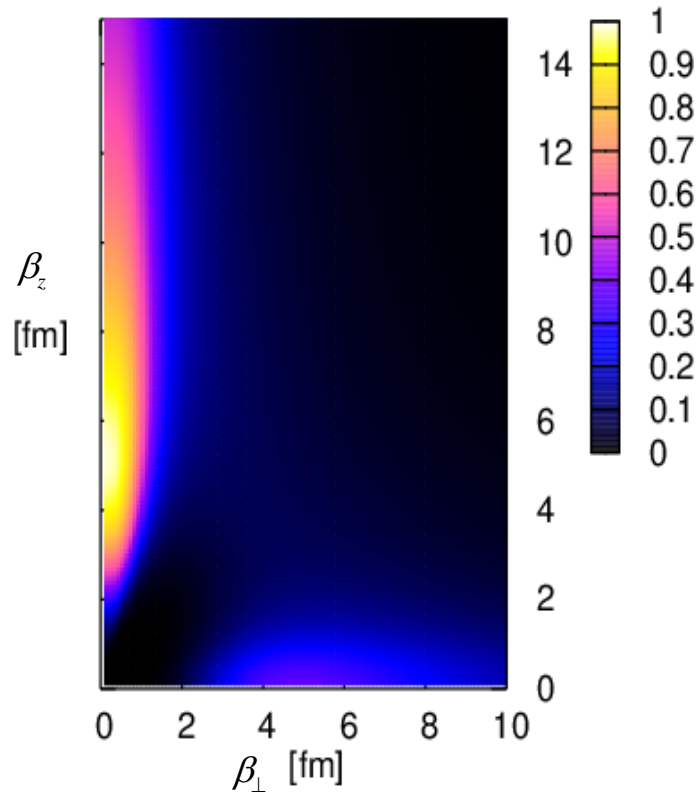
T. Suhara, Y. F. et al., PRL112, 062501 (2014)

$$B_k^2 = b^2 + 2\beta_k^2 \quad (k = x, y, z)$$

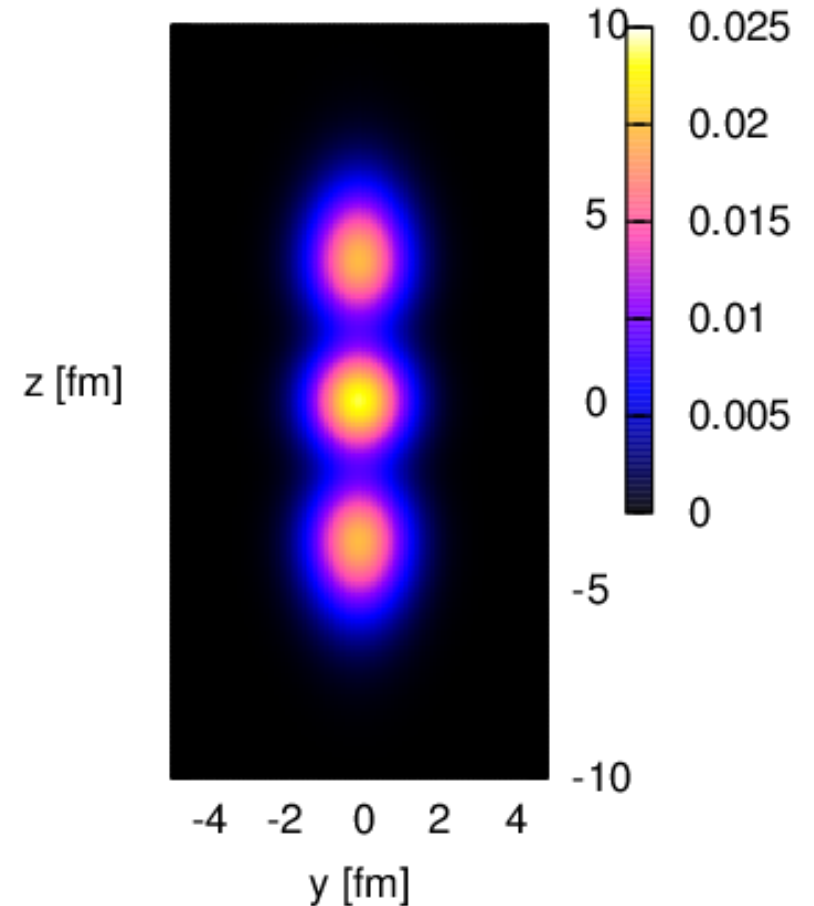
$$\beta_\perp \equiv \beta_x = \beta_y$$



$$O(\beta_\perp, \beta_z) = \left| \left\langle \Phi_{J=0}^{\text{THSR}}(\beta_\perp, \beta_z) \left| \sum_{d_1, d_2} f_\lambda^{(J=0)}(d_1, d_2) \Phi_{J=0}(d_1, d_2) \right. \right\rangle \right|^2$$



Intrinsic density (0.1, 5.1) for β



Maxima

J=0: 0.9873 $\beta=(0.1, 5.1)$

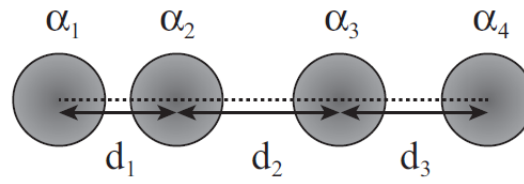
J=2: 0.9887 $\beta=(0.1, 5.4)$

J=4: 0.9806 $\beta=(0.1, 6.6)$

The superposition of 100 Brink w.fs. coincides with one one-dim. THSR !

The squared overlap with one-dim. THSR with single parameter

T. Suhara, Y. F. et al., PRL112, 062501 (2014)

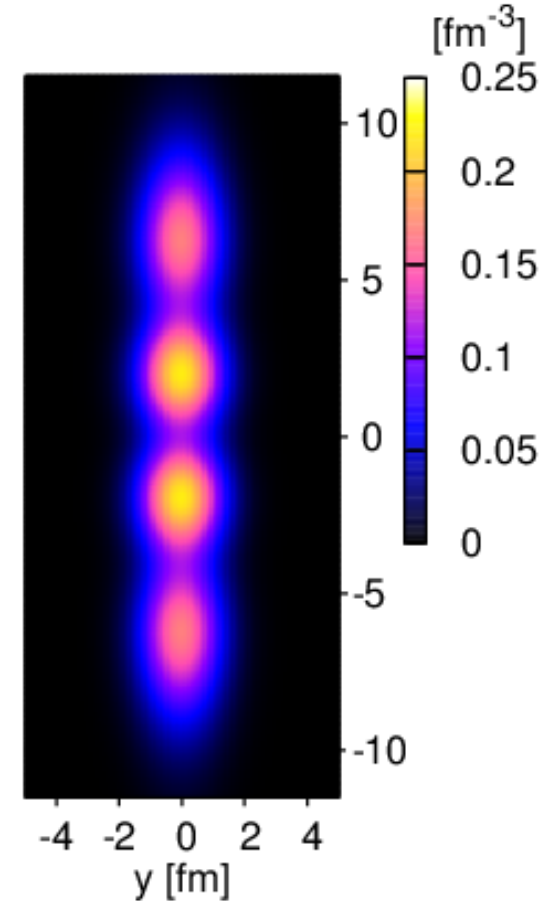
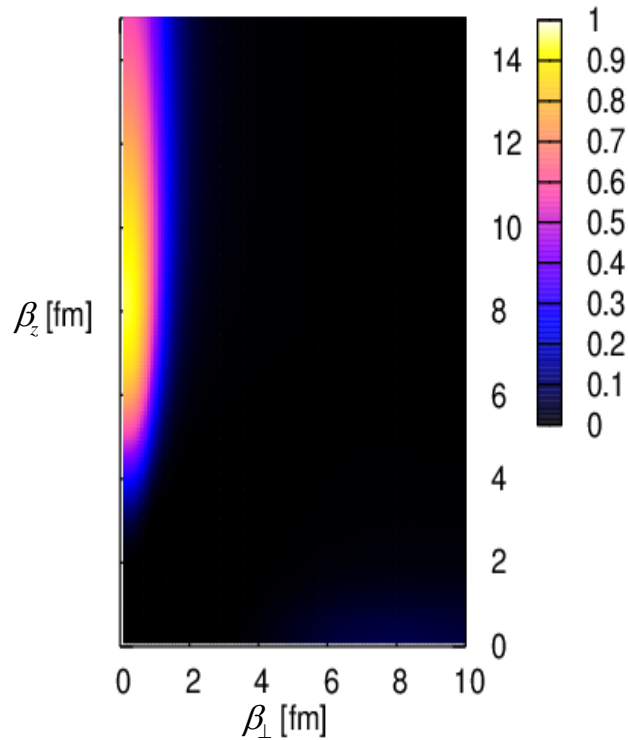


Intrinsic density (0.1, 8.2) for β

$$B_k^2 = b^2 + 2\beta_k^2 \quad (k = x, y, z)$$

$$\beta_{\perp} \equiv \beta_x = \beta_y$$

$$O(\beta_{\perp}, \beta_z) = \left| \left\langle \Phi_{J=0}^{\text{THSR}}(\beta_{\perp}, \beta_z) \left| \sum_{d_1, d_2, d_3} f_{\lambda}^{(J=0)}(d_1, d_2, d_3) \Phi_{J=0}(d_1, d_2, d_3) \right. \right\rangle \right|^2$$



Maxima

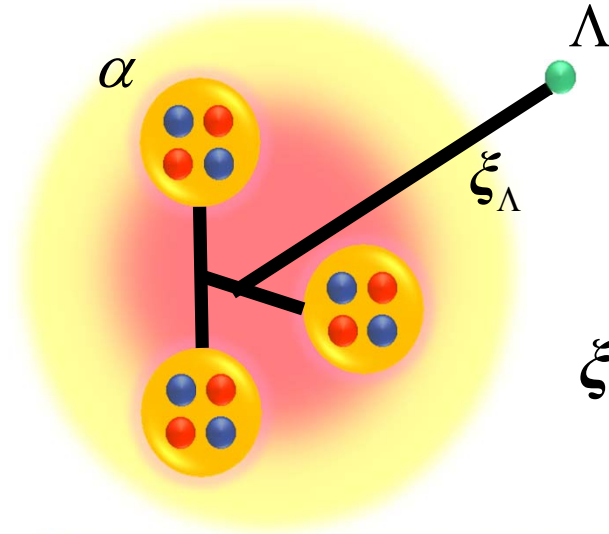
J=0: **0.9440** $\beta=(0.1, 8.2)$

J=2: **0.9417** $\beta=(0.1, 8.4)$

J=4: **0.9307** $\beta=(0.1, 9.0)$

The superposition of 300 Brink w.fs. coincides with one one-dim. THSR !

We make use of the THSR w.f. in the hyperon world.



Hyper-THSR, applied to ${}^9_{\Lambda}\text{Be}$, ${}^{13}_{\Lambda}\text{C}$, ${}^{17}_{\Lambda}\text{O}$, ...

$$\xi_{\Lambda} = r_{\Lambda} - X_C \quad X_C = \frac{r_1 + \dots + r_{4n}}{4n}$$

\hat{P}_I : angular momentum projection operator

$$\Phi_{[I,l]_J}^{\text{Hyper-THSR}}(B_{\perp}, B_z, \kappa) = \mathcal{A} \left\{ \prod_{i=1}^n \hat{P}_I \chi_{3\alpha}^{\text{THSR}}(B_{\perp}, B_z : X_i - X_C) \phi(\alpha_i) \right\} \varphi_{\kappa}^{(l)}(\xi_{\Lambda})$$

$$\chi^{\text{THSR}}(X : B_{\perp}, B_z) = \exp \left(-\frac{2}{B_{\perp}^2} (X_x^2 + X_y^2) - \frac{2}{B_z^2} X_z^2 \right)$$

$$\varphi_{\kappa}^{(l)}(\xi_{\Lambda}) = N_{\kappa,l} \xi_{\Lambda}^l \exp \left(-\frac{\xi_{\Lambda}^2}{\kappa^2} \right) Y_{lm}(\hat{\xi}_{\Lambda})$$

In the present study, $l=0$ only taken into account

*Spatial shrinkage happens when Λ particle is injected in a nucleus.
The corresponding rearrangement effect can be optimally described.*

${}^9_{\Lambda}\text{Be}(0^+, 2^+, 4^+)$ Energy spectra

$\Lambda\text{N}:\text{YNG}$ (ND) interaction

$$\sum_{B'_{\perp}, B'_z} \left\langle \Phi_{[J,0]_J}^{\text{Hyper-THSR}}(B_{\perp}, B_z, \kappa) \left| H - E_{\lambda}(\kappa) \right| \Phi_{[J,0]_J}^{\text{Hyper-THSR}}(B'_{\perp}, B'_z, \kappa) \right\rangle f_{\lambda}(B'_{\perp}, B'_z) = 0$$

$$\Lambda \text{ particle w.f.: } \varphi_{\kappa}^{(l=0)}(\xi_{\Lambda}) = N_{\kappa, l=0} \exp\left(-\frac{\xi_{\Lambda}^2}{\kappa^2}\right) Y_{00}(\hat{\xi}_{\Lambda})$$

$$k_f = 0.962 \text{ fm}^{-1}$$

$$J=0^+$$

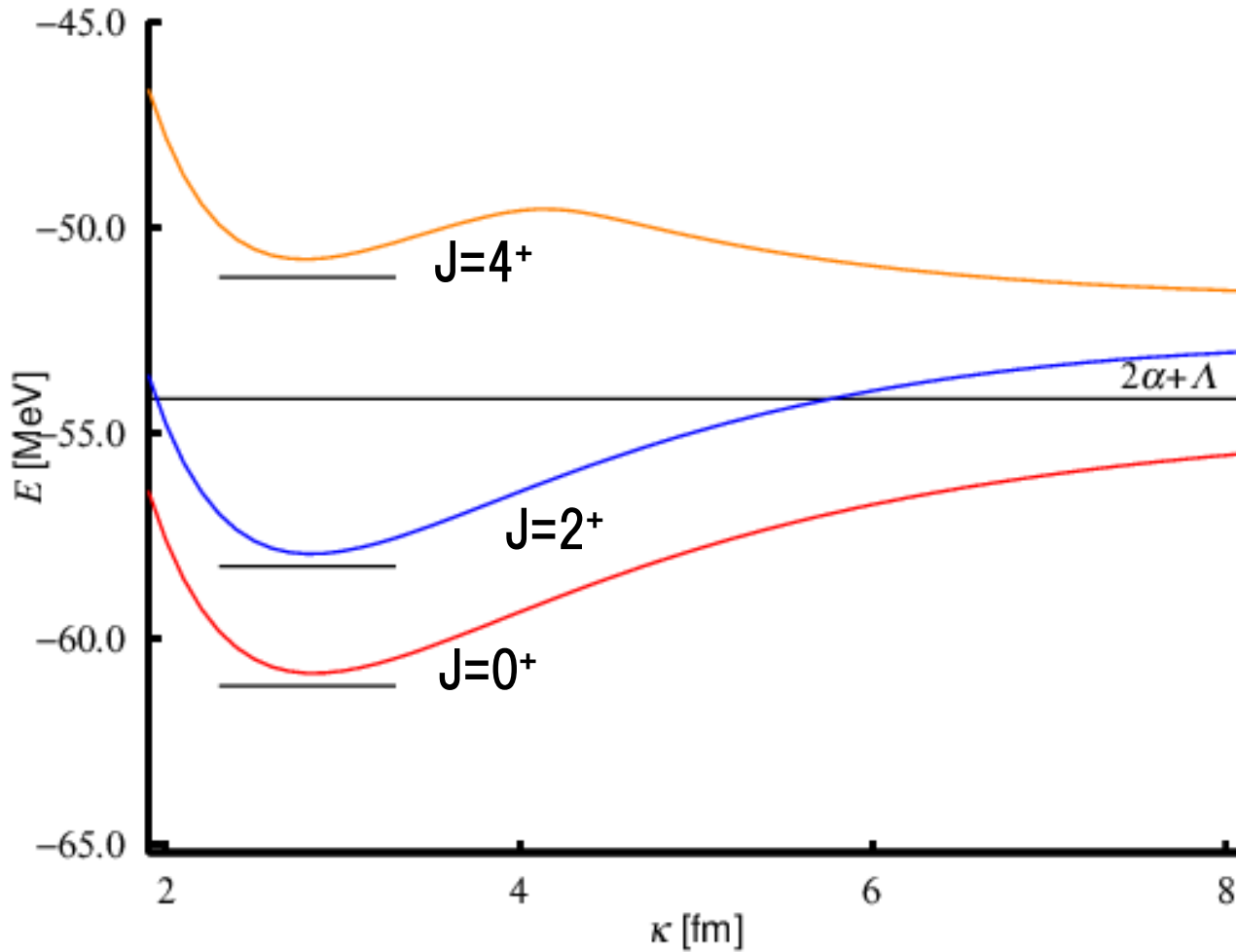
Exp.

Cal.

$$B_{\Lambda} : 6.71 \text{ MeV}$$

$$6.69 \text{ MeV}$$

NN: Volkov No.1 M=0.56
b=1.36 fm

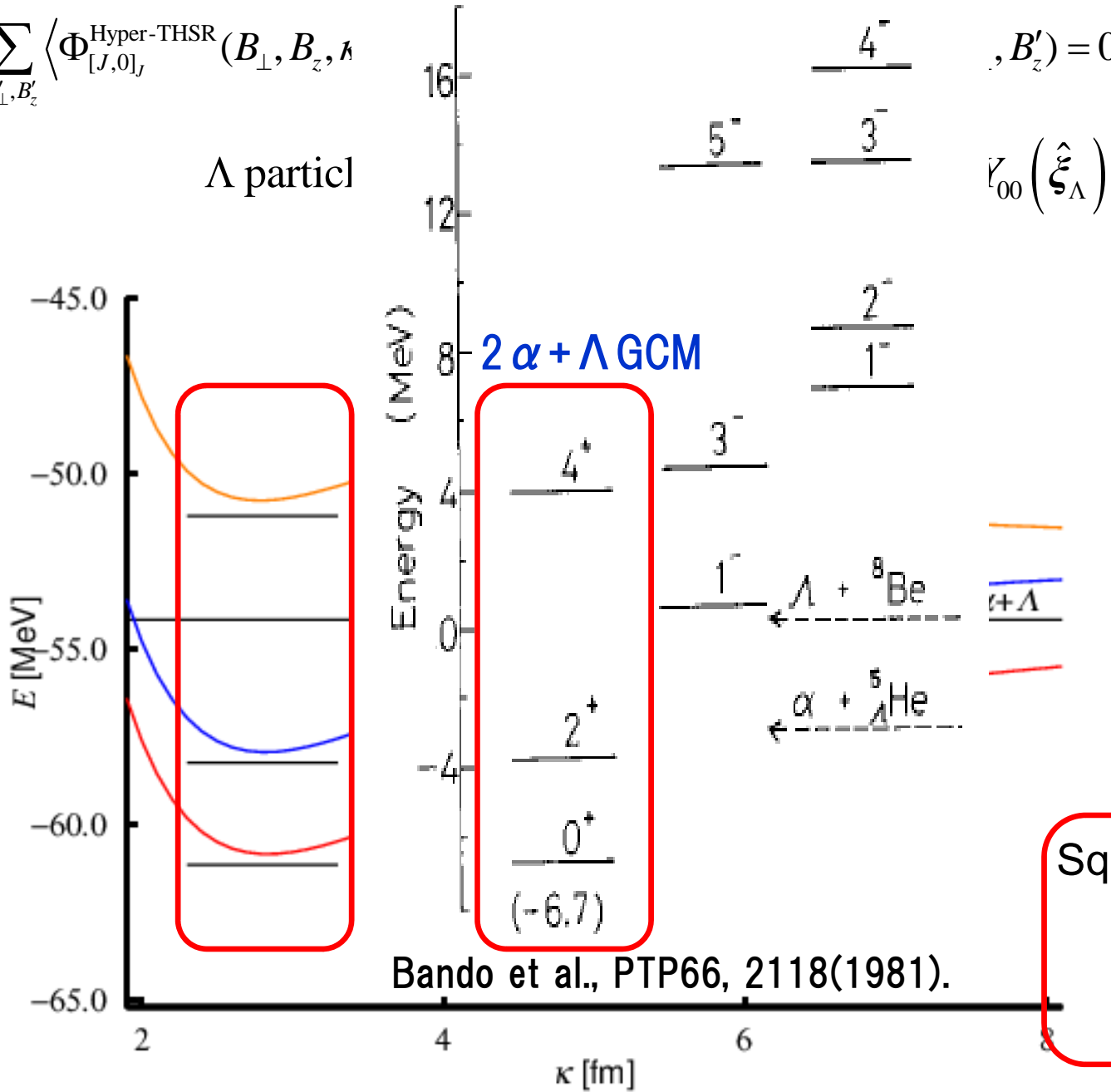


${}^9_{\Lambda}\text{Be}(0^+, 2^+, 4^+)$ Energy spectra

$\Lambda\text{N}:\text{YNG (ND)}$ interaction

$$\sum_{B'_1, B'_2} \langle \Phi_{[J,0]_J}^{\text{Hyper-THSR}}(B_{\perp}, B_z, \hbar) \rangle$$

Λ particle



$$k_f = 0.962 \text{ fm}^{-1}$$

$$J = 0^+$$

Exp. Cal.

$$B_{\Lambda} : 6.71 \text{ MeV} \quad 6.69 \text{ MeV}$$

NN: Volkov No.1 $M=0.56$
 $b=1.36 \text{ fm}$

Squared overlap with $2\alpha + \Lambda$ GCM

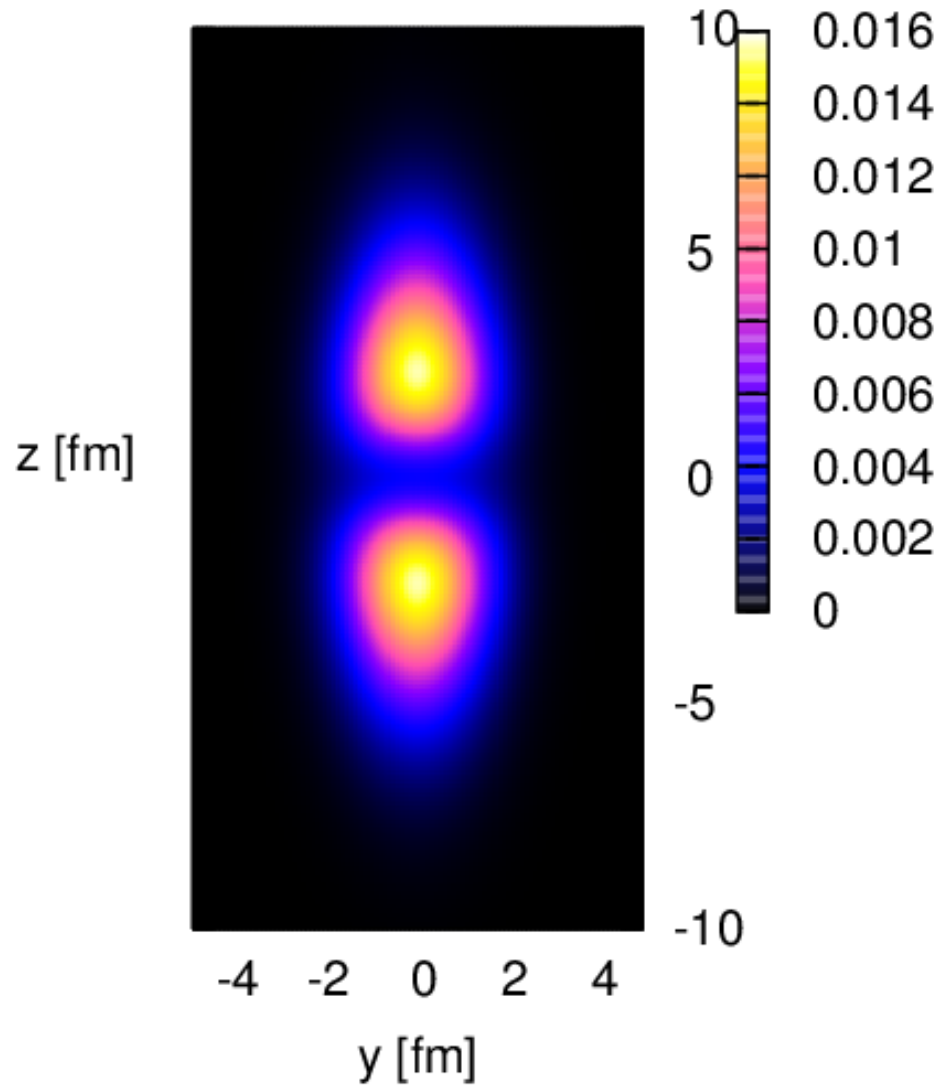
$$J=0: 0.992 \quad \beta=(0.1, 3.3)$$

$$J=2: 0.994 \quad \beta=(0.1, 3.0)$$

Bando et al., PTP66, 2118(1981).

Comparison of intrinsic density between ${}^8\text{Be}(0^+)$ & ${}^9_{\Lambda}\text{Be}(0^+)$

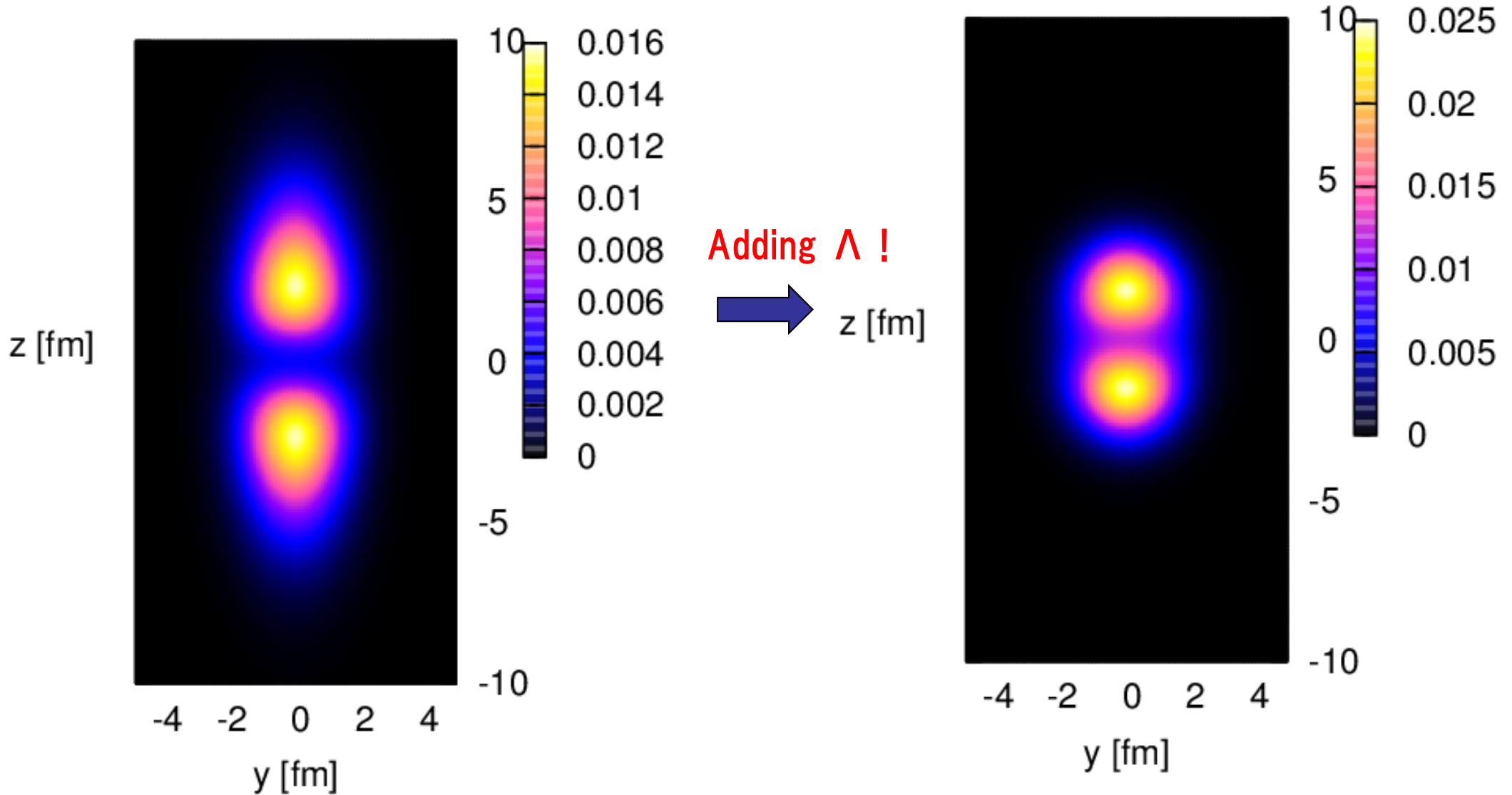
${}^8\text{Be}(0^+)$ $R_{\text{rms}}=2.9$ fm



Comparison of intrinsic density between ${}^8\text{Be}(0^+)$ & ${}^9_{\Lambda}\text{Be}(0^+)$

${}^8\text{Be}(0^+)$ $R_{\text{rms}}=2.9$ fm

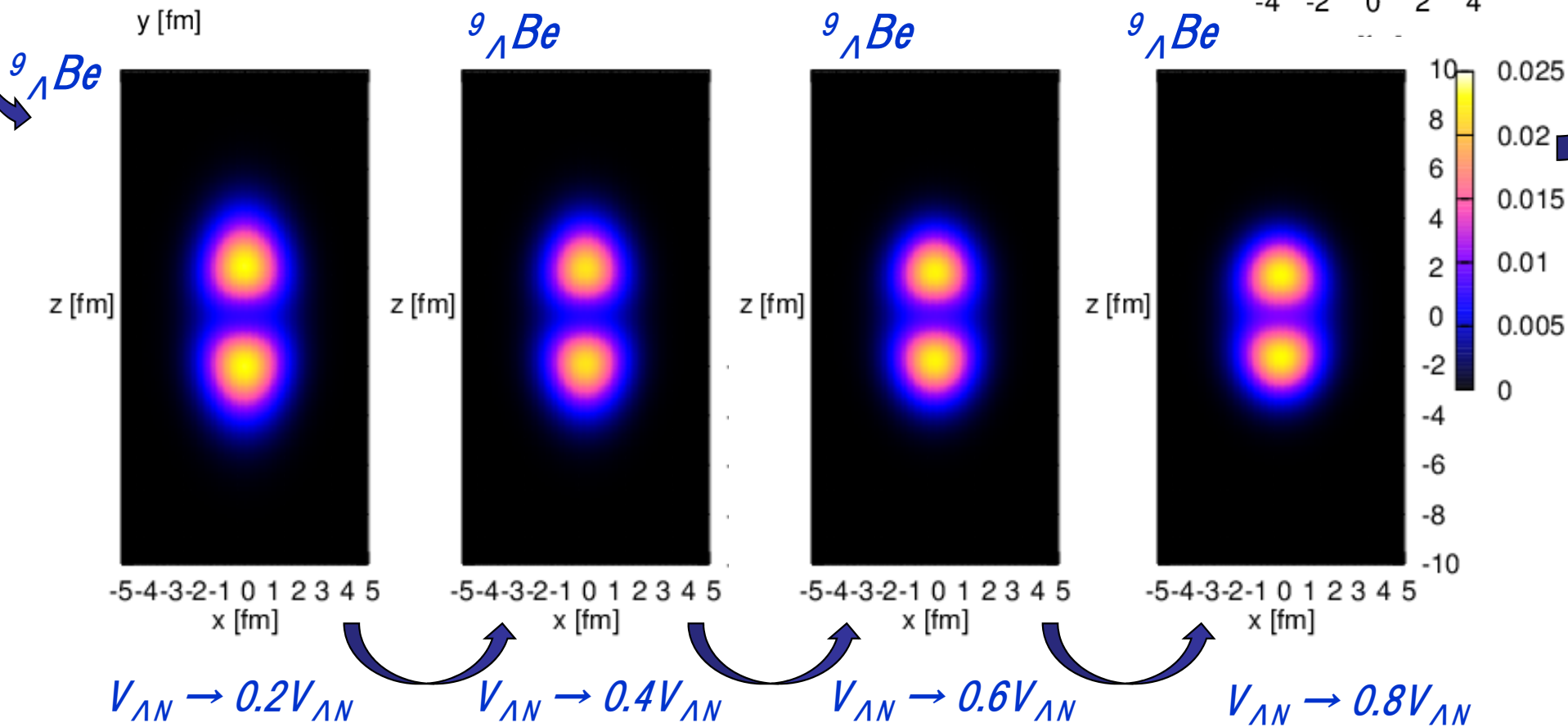
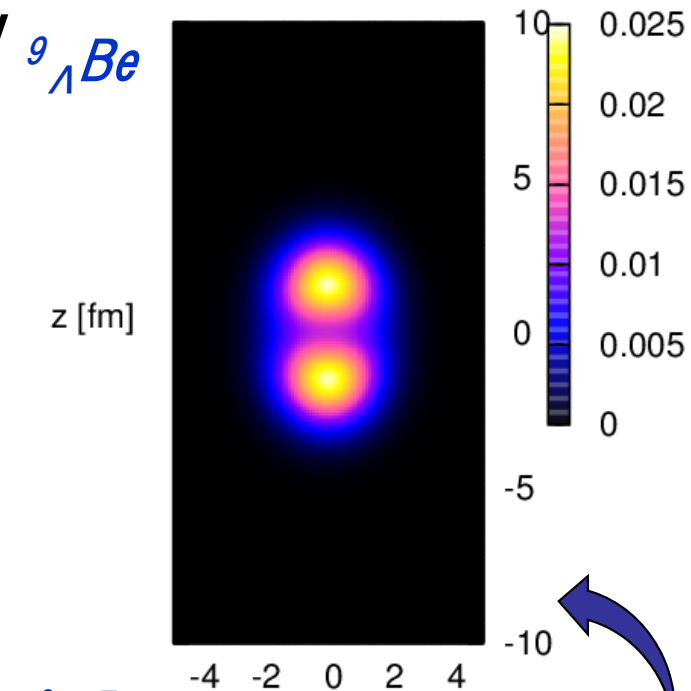
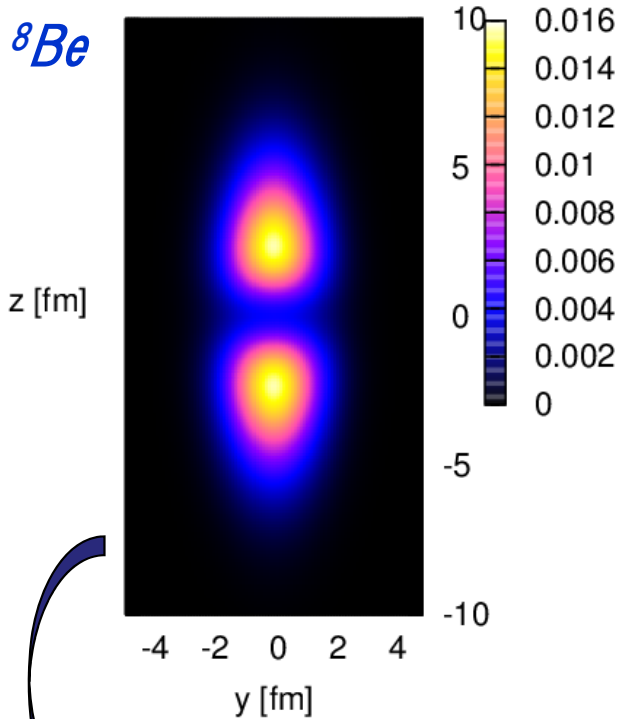
${}^9_{\Lambda}\text{Be}(0^+)$ $R_{\text{rms}}=2.34$ fm



2 α structure still survives in the normal density !

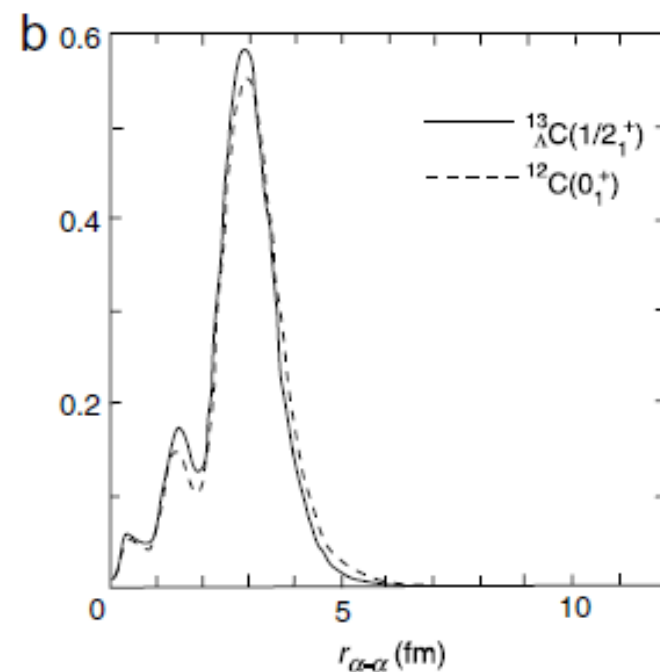
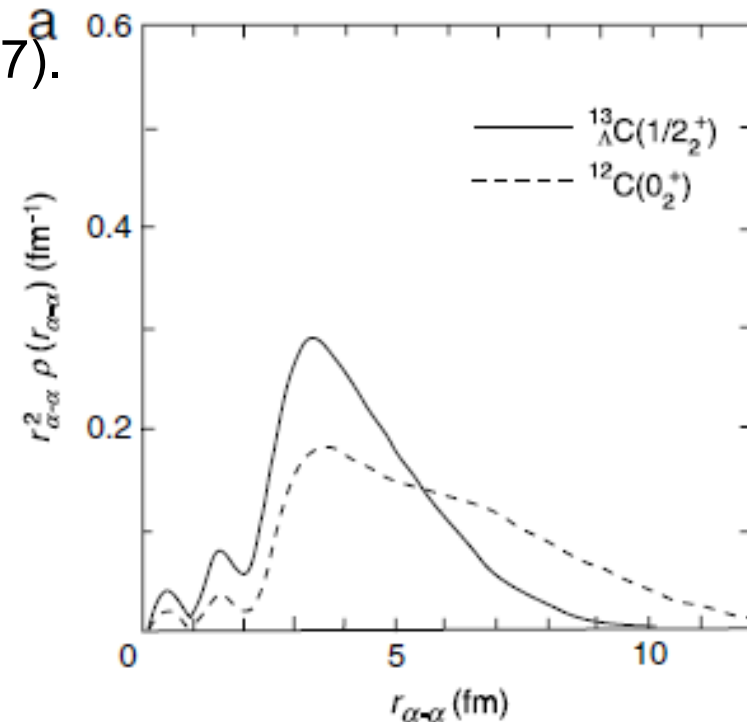
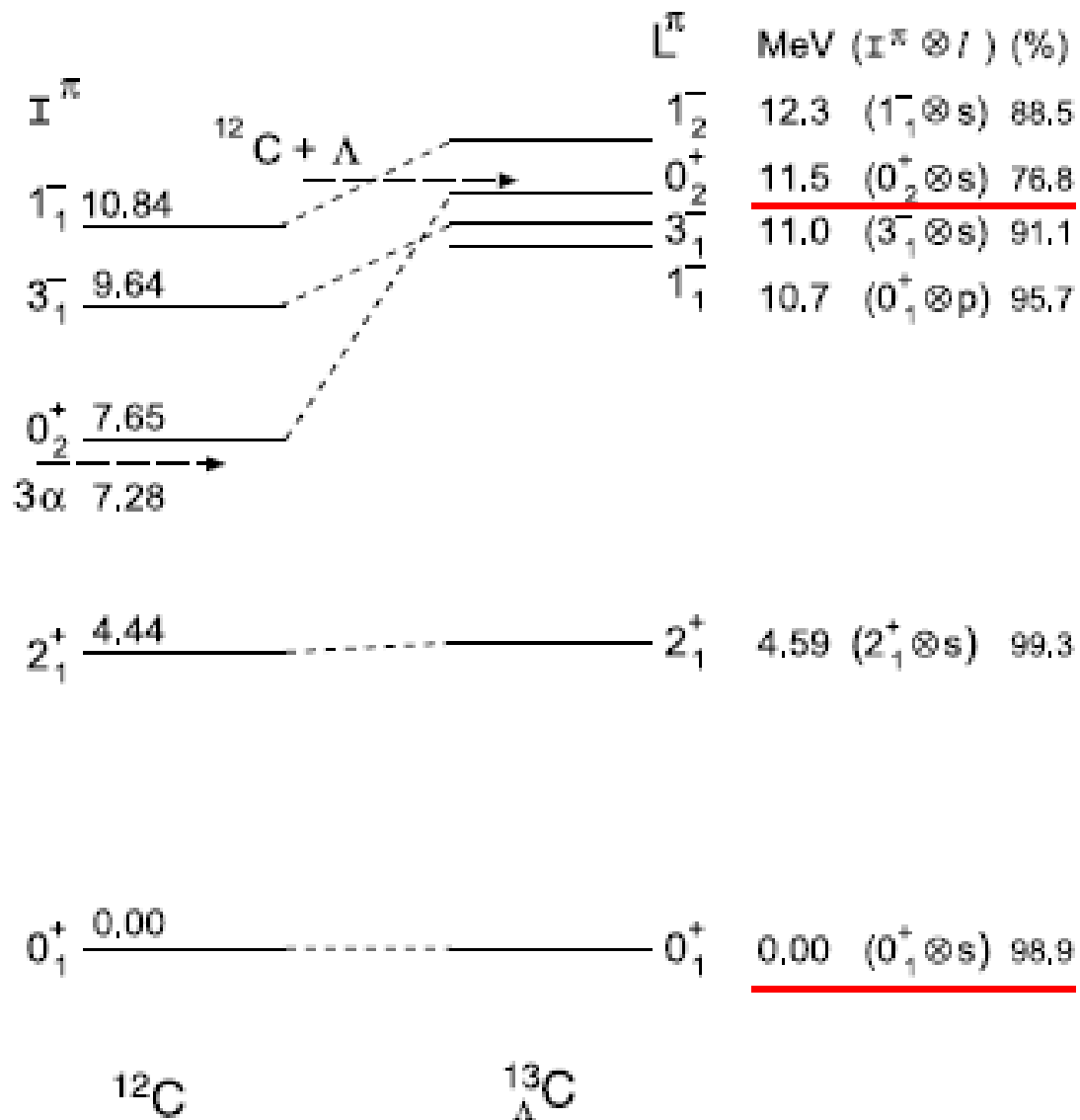
Λ particle does not disturb the strong Pauli repulsion of α - α
Pauli principle plays a crucial role in producing clusters.

Structural change as ΛN interaction increases



$3\alpha + \Lambda$ OCM by Hiyama et al. YNG (JA) interaction

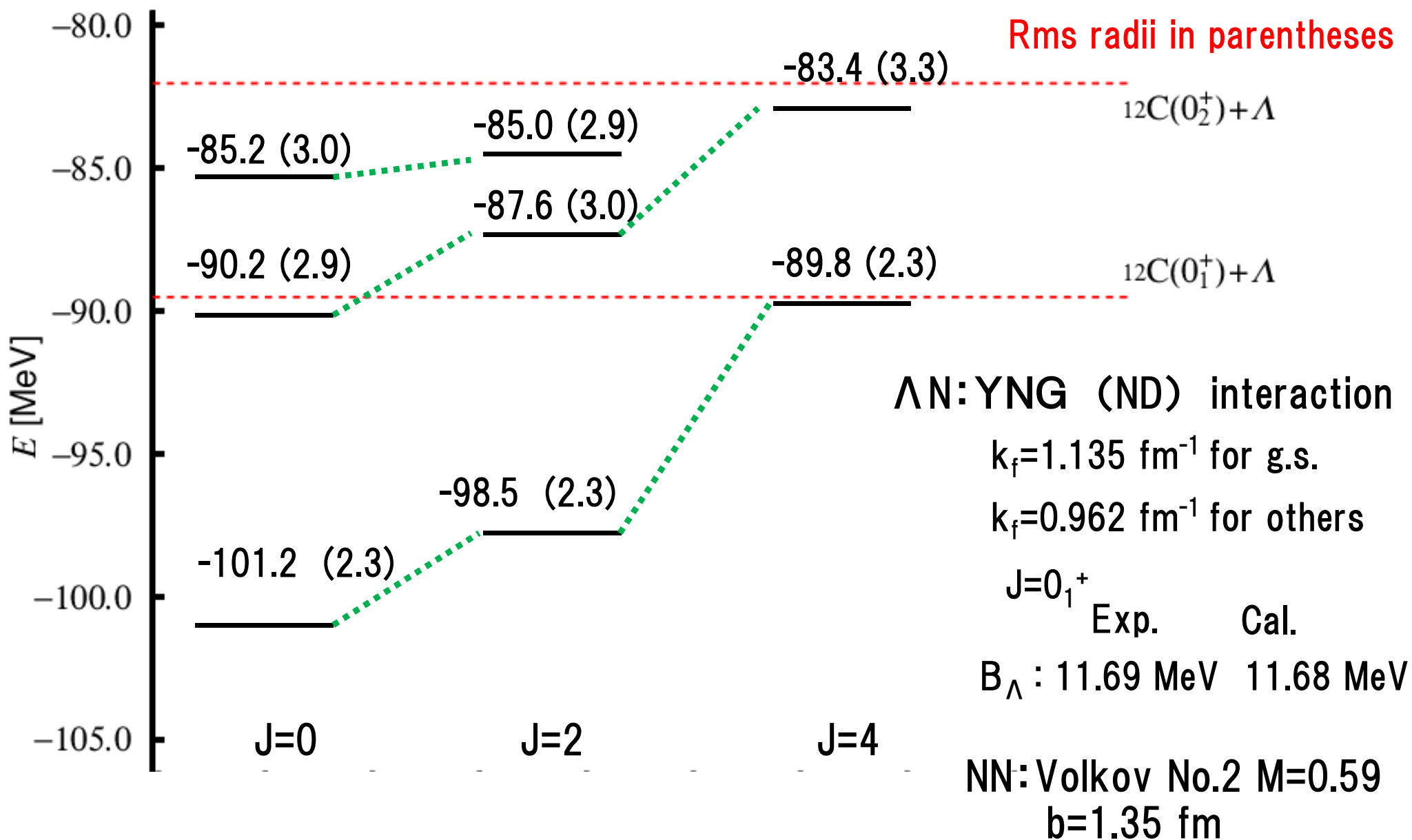
E. Hiyama et al., PTP 97, 881 (1997).



Spatial shrinkage is seen.

Energy of $^{13}_{\Lambda}\text{C}(0^+, 2^+, 4^+)$

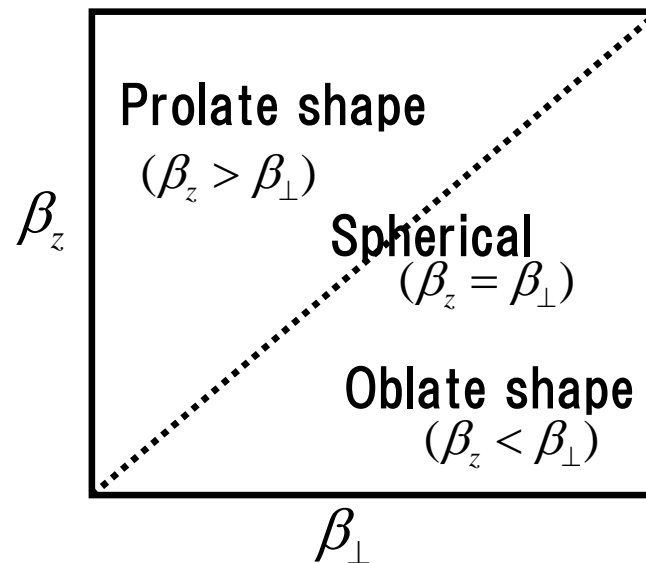
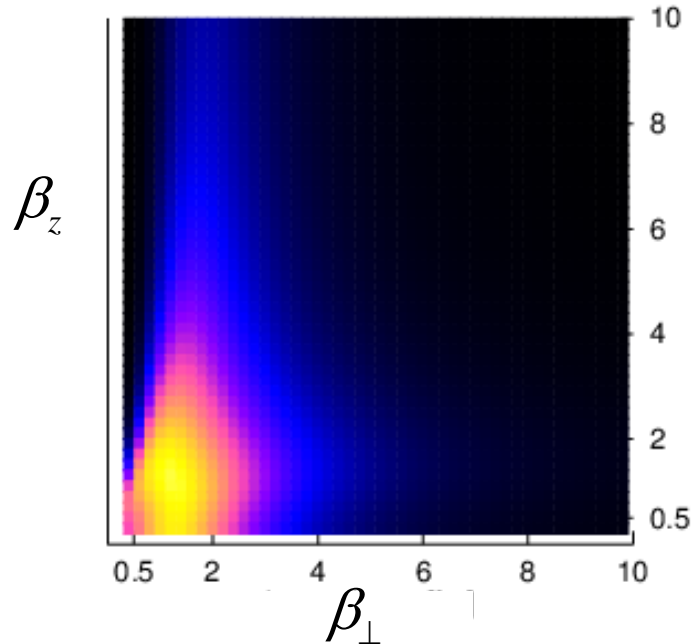
$$\sum_{B'_{\perp}, B'_z, \kappa'} \left\langle \Phi_{[J,0]_J}^{\text{Hyper-THSR}}(B_{\perp}, B_z, \kappa) \left| H - E_{\lambda} \right| \Phi_{[J,0]_J}^{\text{Hyper-THSR}}(B'_{\perp}, B'_z, \kappa') \right\rangle f_{\lambda}(B'_{\perp}, B'_z, \kappa') = 0$$



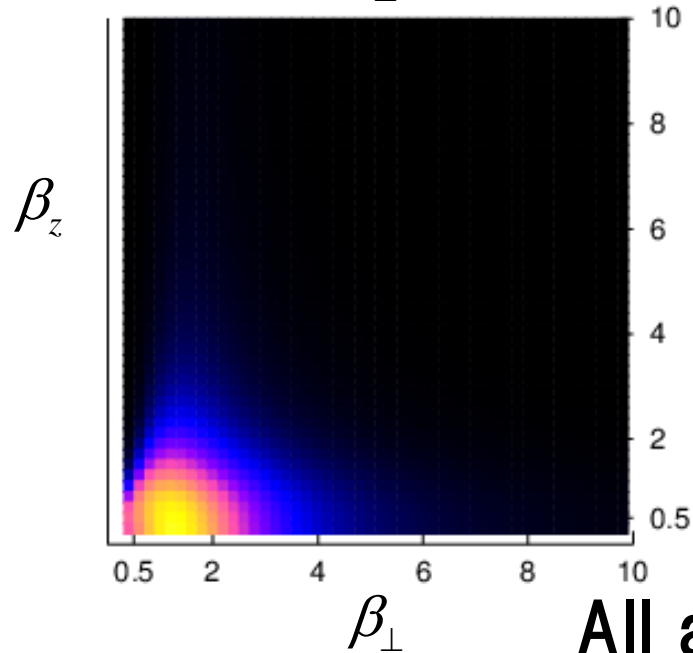
Squared overlap surfaces for 0_1^+ , 2_1^+ , 4_1^+

$$O(\beta_{\perp}, \beta_z, \kappa) = \left| \sum_{D', D''} \left\langle \Phi_{[J,0]_J}^{\text{Hyper-THSR}}(B_{\perp}, B_z, \kappa) \middle| \Phi_{[J,0]_J}^{\text{Hyper-THSR}}(B'_{\perp}, B'_z, \kappa) \right\rangle f_{\lambda}(B'_{\perp}, B'_z, \kappa) \right|^2$$

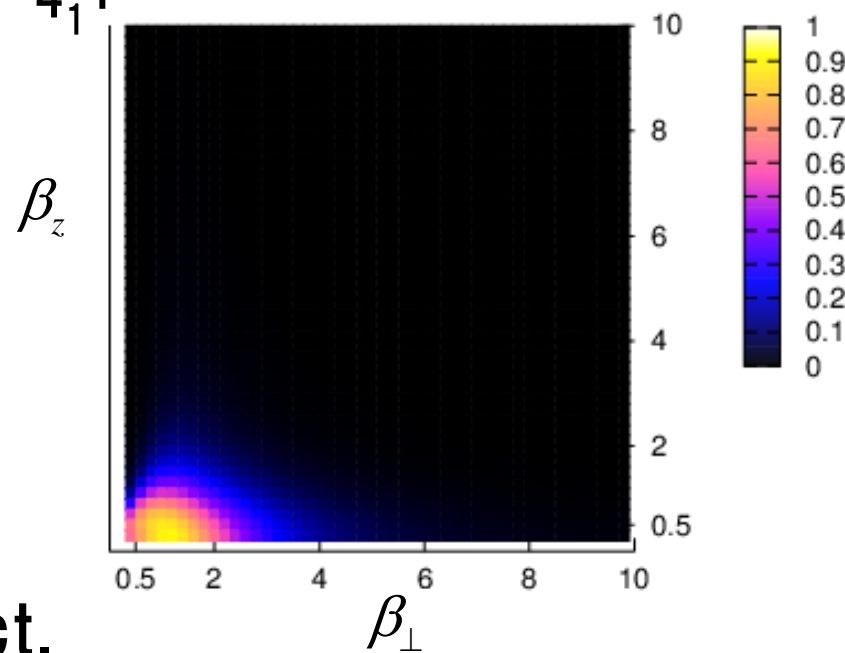
0_1^+



2_1^+



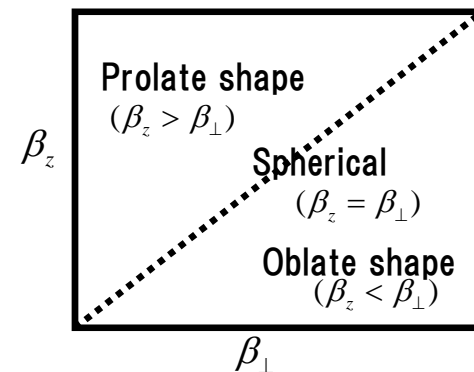
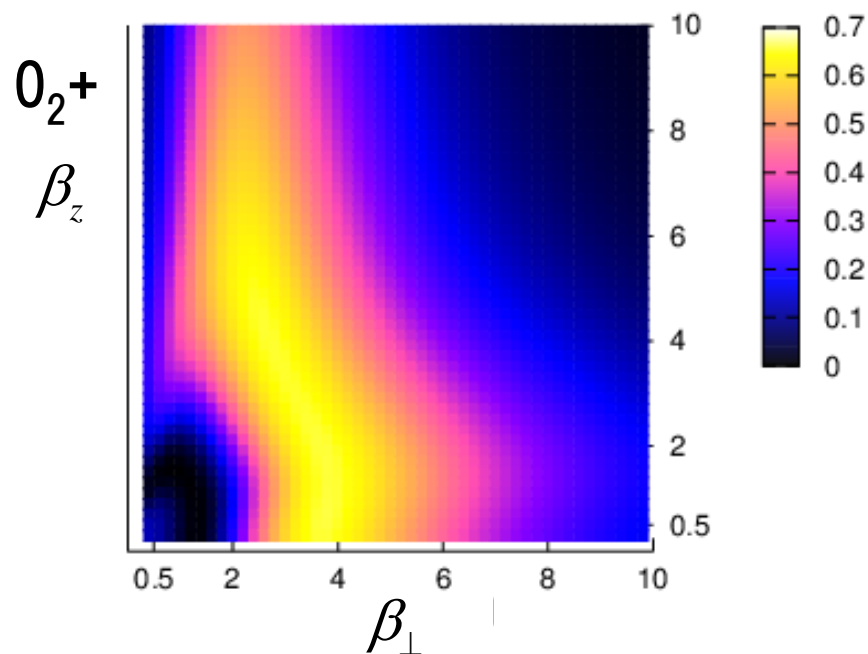
4_1^+



All are compact.

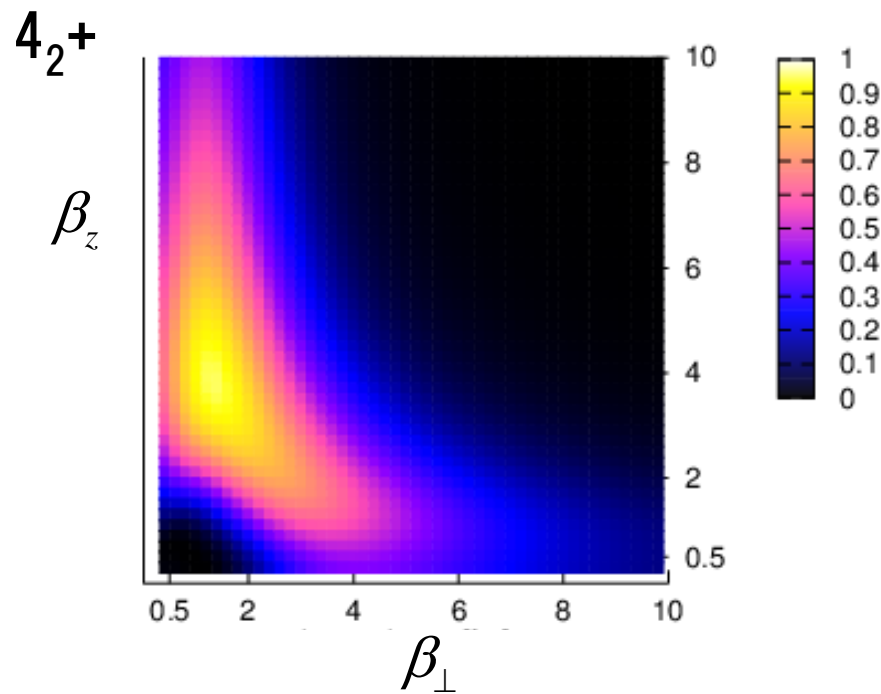
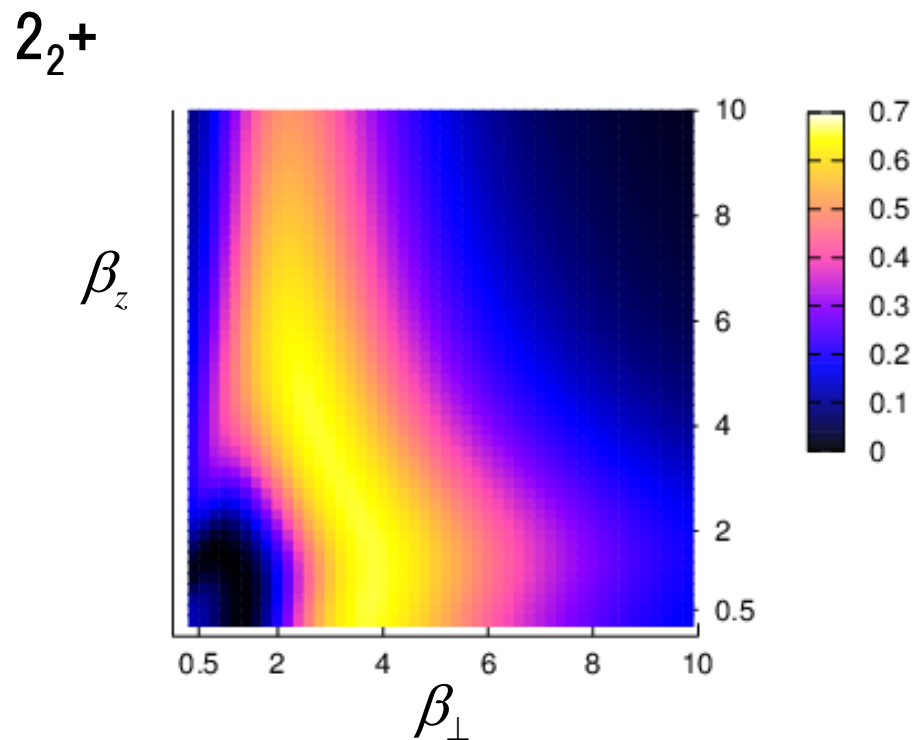
Squared overlap surfaces for 0_2^+ , 2_2^+ , 4_2^+

Family of the Hoyle state



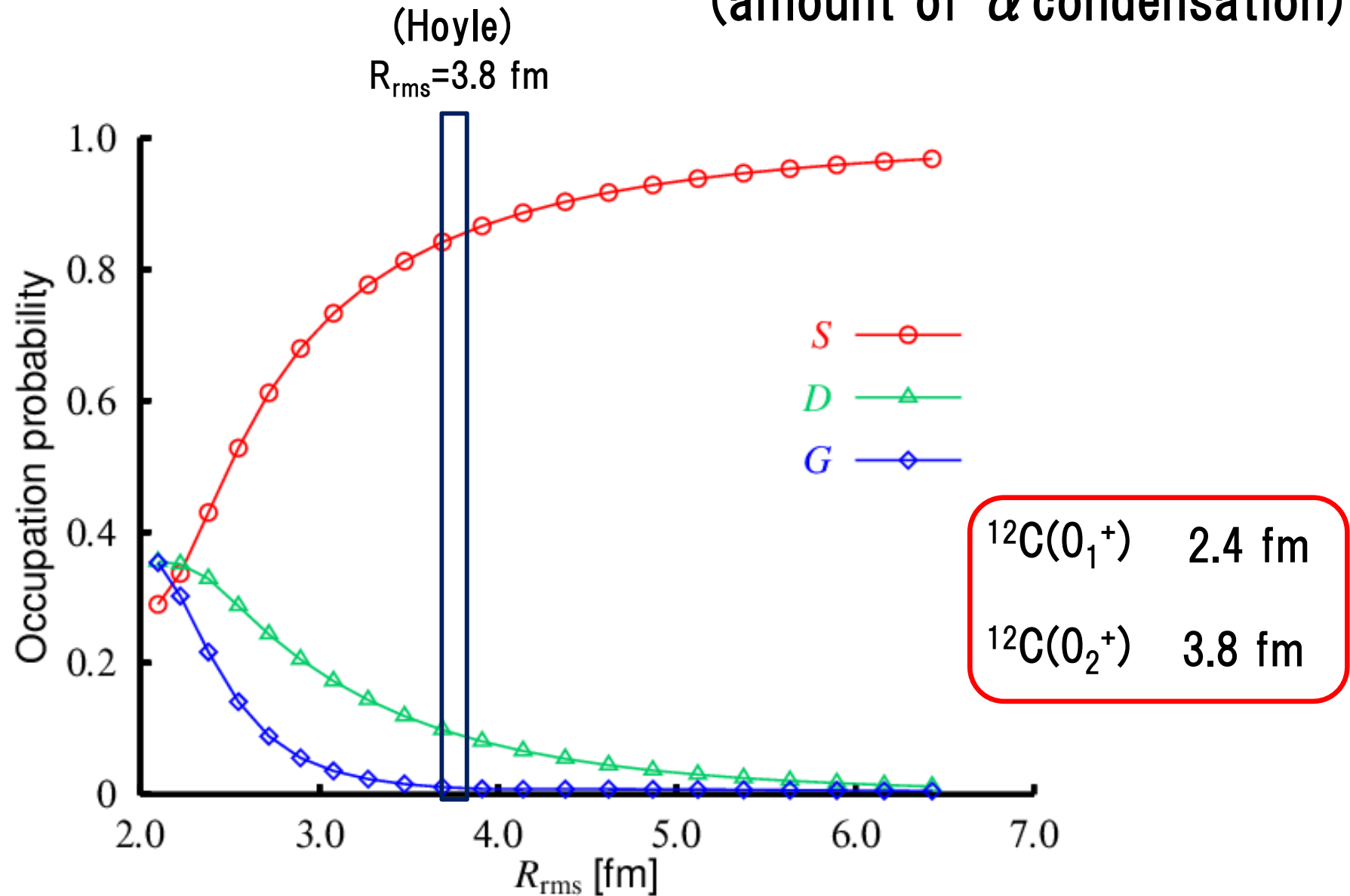
**Dilute density like a gas
All do not have definite shape.**

Note: The Hoyle state band is not yet confirmed in ^{12}C .



Size dependence of occupation probability

(amount of α condensation)

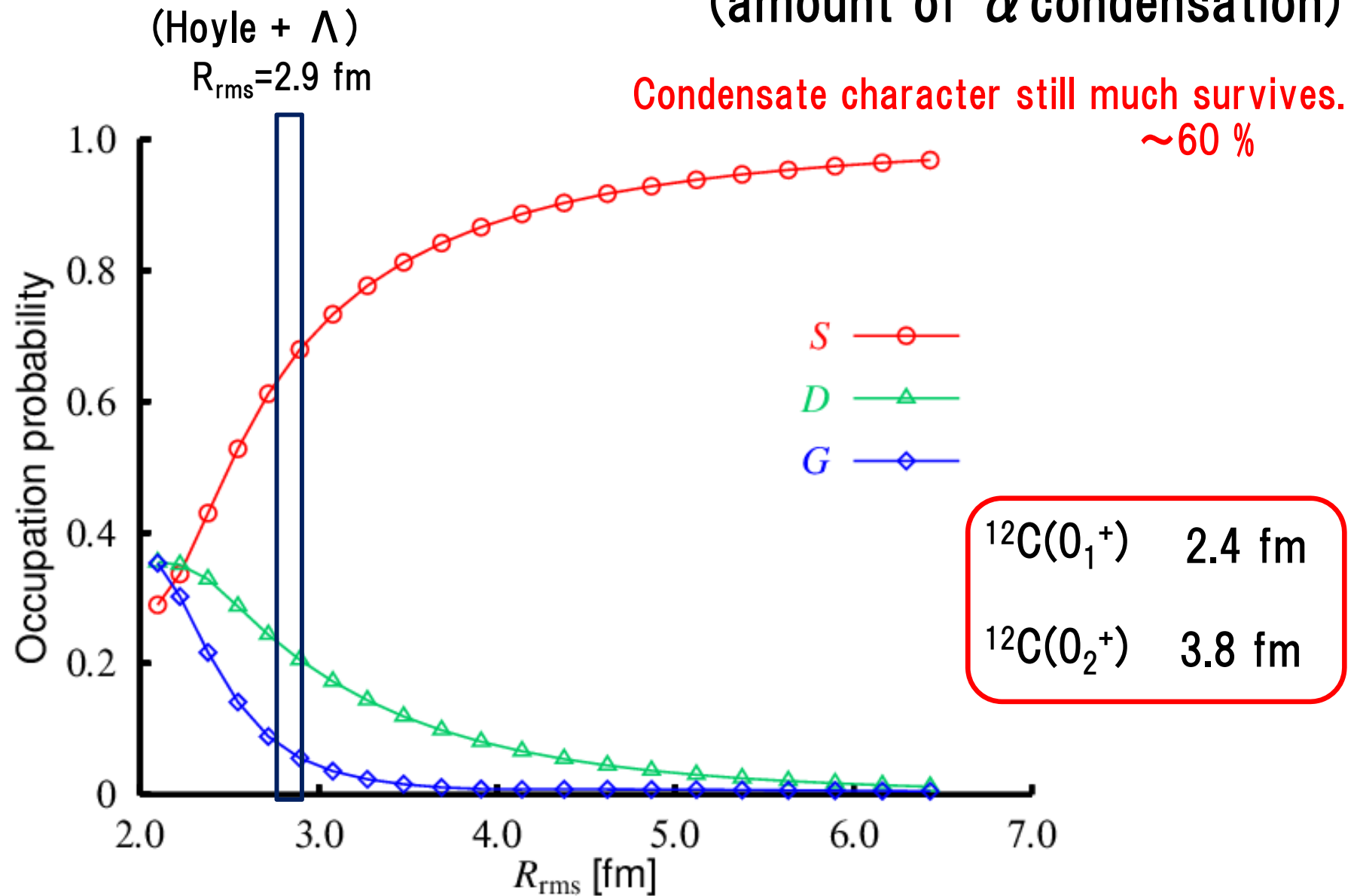


$R_{\text{rms}} < 2.5$ fm: Alpha's are resolved due to the antisymmetrization.

$R_{\text{rms}} \rightarrow$ large: Alpha's occupy a single S -orbit only.

Size dependence of occupation probability

(amount of α condensation)

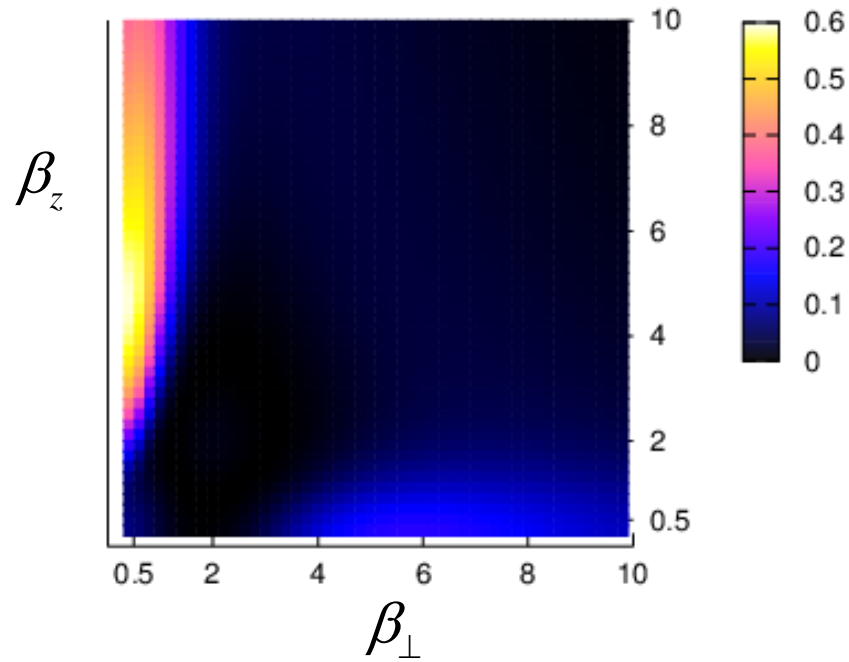


$R_{\text{rms}} < 2.5$ fm: Alpha's are resolved due to the antisymmetrization.

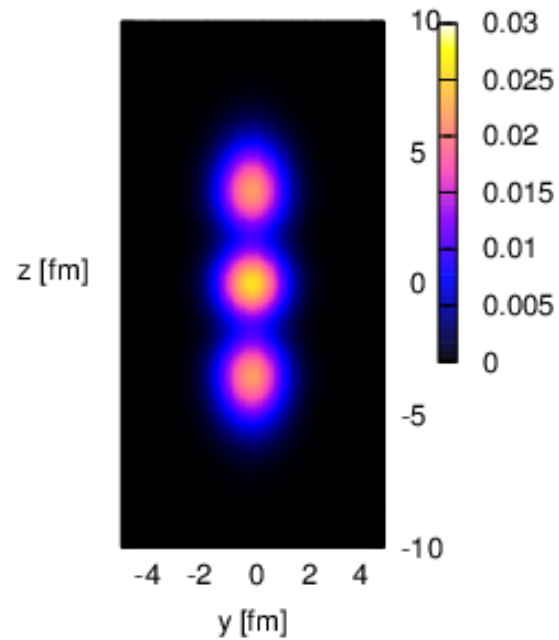
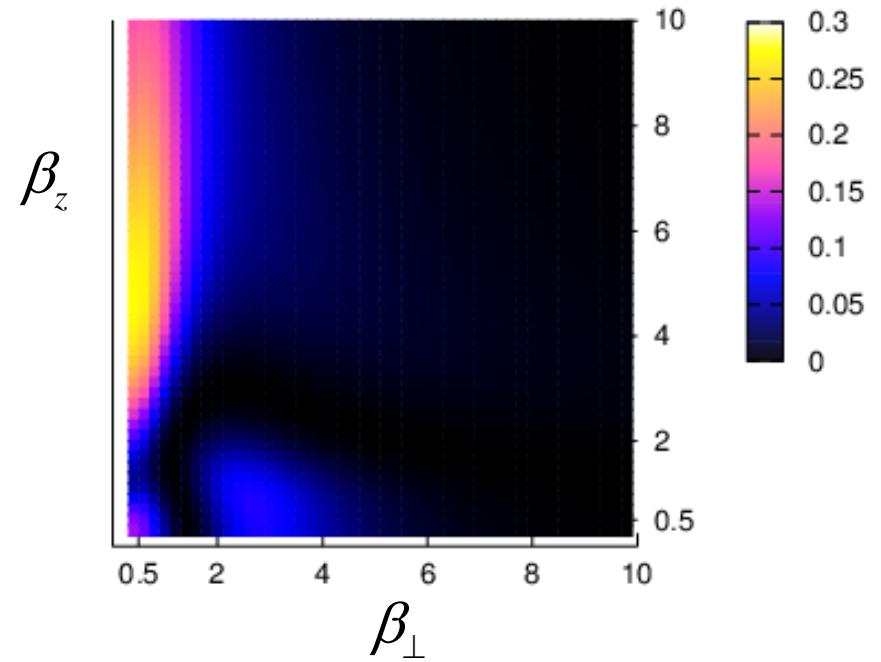
$R_{\text{rms}} \rightarrow$ large: Alpha's occupy a single S -orbit only.

1 dim.-like linear-chain band

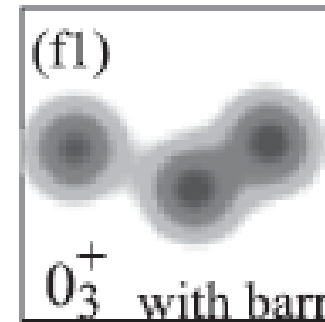
0_3^+



2_3^+



^{12}C : 0_3^+ state (or 0_4^+)



AMD by En'yo, (PTP117, 655(2007)).
and FMD by T. Neff.

Summary

Based on the fact that THSR w.f. succeeded in describing gas-like states (${}^8\text{Be}$, ${}^{12}\text{C}$) and even for ordinary cluster states (${}^{20}\text{Ne}$ and g.s. ${}^{12}\text{C}$)



The linear chain states which we have imagined are one-dim. gases of alphas to be described by THSR.



Hyper-THSR w.f. is introduced to apply it to Λ hypernuclei.
very promising way of describing light hypernuclei

- ${}^9_{\Lambda}\text{Be}$: The ground rotational band is successfully reproduced.

Large shrinkage effect: 2 alpha structures still survive.

Powerful effect of Pauli principle.

- ${}^{13}_{\Lambda}\text{C}$: One dimensional gas of three alphas, as the 0_3^+ , 2_3^+ states.
More straightly aligned than in ${}^{12}\text{C}(0_3^+)$

Thanks

to my Collaborators

Bo Zhou (Nanjing U.)

Zhongzhou Ren (Nanjing U.)

Chang Xu (Nanjing U.)

Taiichi Yamada (Kanto Gakuin U.)

Tadahiro Suhara (Matsue)

Hisashi Horiuchi (RCNP)

Akihiro Tohsaki (RCNP)

Peter Schuck (IPN, Orsay)

Gerd Röpke (Rostock U.)

Emiko Hiyama (RIKEN)

Kiyomi Ikeda (RIKEN)

and for your attention.